Alma Mater Studiorum · Università di Bologna

Scuola di Scienze
Dipartimento di Fisica e Astronomia
Corso di Laurea in Fisica

Results of the ageing campaign of the photomultiplier Hamamatsu R760

Relatore:
Dott. Fabio Ferrari

Correlatore:
Prof. Angelo Carbone

Presentata da:
Alberto Bellavista

Anno Accademico 2021/2022

Abstract

Il guadagno di un PMT è il fattore di amplificazione tra la corrente generata dal fotocatodo e quella finale dell'anodo. Quando un PMT è soggetto a una sorgente luminosa per lunghi periodi di tempo (processo noto come "invecchiamento"), il suo guadagno tende a diminuire.

In questa tesi sono riportati i risultati della campagna di invecchiamento di un fotomoltiplicatore Hamamatsu R760. In particolare, è stato studiato come variasse il guadagno in funzione della carica integrata dal PMT tramite due principali tipi di misure: quella del guadagno assoluto, che consiste in singole misure di guadagno nella condizione di emissione di un singolo fotoelettrone alla volta, e quelle di guadagno relativo, le quali hanno permesso di studiare la dipendenza tra guadagno e voltaggio applicato al PMT.

Il PMT in esame è stato fatto invecchiare fino a una carica integrata totale pari a 342 C. Una volta raggiunti i 282 C, è stato spento per 20 giorni, in modo da studiare l'eventuale capacità di recuperare guadagno durante i periodi di inattività.

É stata osservata una rapida decrescita del guadagno nei primi 40 C integrati, cominciando da $7.79 \cdot 10^6$ fino a un valore pari a $1.68 \cdot 10^6$, seguita da oscillazioni minori attorno a una decrescita lineare media. Dopo il periodo di inattività non è stato rilevato alcun recupero significativo di guadagno.

Il guadagno del PMT dipende dal voltaggio applicato tramite una legge a potenza, i cui parametri sono stati misurati. In particolare, gli esponenti di tale relazione sono stati soggetti a una decrescita rapida iniziale (nei primi 40 C di carica integrata), seguita da una stabilizzazione. Inoltre, sono stati ricavati i valori di tensione da applicare al PMT per mantenere il guadagno a un valore costante di $1.5 \cdot 10^5$ in funzione della carica integrata. Questo valore è stato scelto come punto di lavoro per il rivelatore PLUME installato nell'esperimento LHCb, che utilizzerà questo tipo di PMT per la sua campagna di misure.

Abstract

The PMT gain is the amplification factor between the initial PMT photocathode current and the final anode current. When subjected to a source of light for long periods of time (the so-called "ageing") the gain tends to diminish.

In this thesis, the results of the ageing campaign of a Hamamatsu R760 PMT are presented. In particular, a variation of the gain as a function of the charge integrated by the photomultiplier tube under study has been studied. Two main experimental procedures have been employed: through the absolute gain measurements, which consist of single gain measurements in the single photoelectron condition, the decrease of the gain during the ageing period has been observed; while the relative gain ones allowed the dependence of the gain from the alimenting voltage of the PMT to be investigated.

During this ageing campaign, the PMT under study reached 342 C of integrated charge, with a non-operating period of 20 days at 282 C. The purpose of such period was to study a possible gain recovery.

The absolute gain showed a strong decrease during the integration of the first 40 C, starting from $7.79 \cdot 10^6$ and reaching a value of $1.68 \cdot 10^6$. During the following days, the gain has been only subjected to small fluctuations around a mean linear decrease. There was not any relevant gain recovery after the non-operating period.

The relation between the PMT gain and its alimenting voltage is a power law. Through the relative method, the exponent parameters of such power law have been obtained. As for the absolute gain, they show a strong initial decrease, followed by a stabilization. Furthermore, the high voltage required to maintain the gain at a fixed value of $1.5 \cdot 10^5$ (as a function of the integrated charge) has been measured. This value has been chosen as working point for the PLUME detector installed in the LHCb experiment, which will use this PMT model during its operation.

Contents

List of Figures

List of Tables

Introduction

Photomultiplier tubes, or PMTs for short, are very sensitive photons detectors. They are used in many fields of study to detect incoming electromagnetic radiation in the near-infrared, visible and ultraviolet ranges.

When a PMT is illuminated for long periods of time, some of its operational properties might change. This process is called "ageing" and in general it can affect the gain and the sensitivity of the PMT.

In this thesis, the measurements and the results of the ageing campaign of a Hamamatsu R760 PMT will be presented and discussed. In particular, the variation of the gain as a function of the charge integrated by the PMT is studied by following two main procedures: the absolute gain measurements and the relative gain measurements. The campaign also featured a recovery period during which the ageing was stopped in order to study a possible gain recovery. The thesis is organised as follows.

Chapter 1 provides an overview of the main features of photomultiplier tubes (and the characteristics of the Hamamatsu R760 PMT), their structure and the physical processes behind their functioning, focusing on the description of the photoelectric effect, the quantum efficiency and the PMT gain. Finally, a brief description of the PMT ageing process and its causes is provided.

In Chapter 2 the experimental setup used in the ageing campaign is described and illustrated. Then, the time structure of the campaign is presented.

Chapter 3 contains the description of the performed measurements. Here, the absolute gain measurements are reported and then the relative gain ones are presented. Also, a detailed description of the single photoelectron condition (S.P.E.) reached during the measurements sessions is presented.

Chapter 4 describes the ageing campaign results both for the absolute and the relative gain measurements. In particular, it focuses on the relation between the PMT gain and its supply voltage.

Finally, conclusions are drawn about the results obtained in the ageing campaign.

Chapter 1

Photomultiplier tubes

Photomultiplier tubes are the most commonly used detectors for photons in experimental particle physics. Since the development of the first photocathodes and secondary emission multipliers (*i.e.* dynode systems) between the last years of the 19th century and the beginning of the 20th century, their technology has been making rapid progresses, increasing the current amplification factor (*i.e.* the PMT gain) [1]. The purpose of photomultipliers is to detect and reveal light pulses by creating an electric current thanks to the so-called "photoelectric effect". The PMT under study in this measurements campaign is a photomultiplier tube Hamamatsu R760 [2].

In this chapter, the PMTs main features are discussed. First, in Sec. 1.1, the physics fundamentals behind the operating principles of a PMT are briefly exposed, focusing on the "photoelectric effect". Then, the structure of a PMT is illustrated and the functioning of its different parts is described. The PMT quantum efficiency and gain, which are two of the main operational properties of a photomultiplier tube, are also presented. Finally, Sec. 1.6 provides a focus on the ageing process of a PMT and its main causes.

1.1 Physics of a PMT

1.1.1 Photons interaction with matter

Photons are particles with no mass and no electric charge. The interaction between photons and matter is a probabilistic process which mainly depends on the light frequency (*i.e.* the photons energy) and the atomic number and density of the absorbing material. Considering photons composing X-rays and γ-rays radiation, there are three main types of interaction with matter:

- pair production;
- Thomson and Rayleigh scattering;
- photoelectric effect.

The first one consists of the creation of an electron-positron pair from an incident photon, which must have an energy at least equal to two electron masses or higher. The Thomson and Rayleigh scattering concern the cases in which the incident photon is elastically scattered by a charged particle, maintaining its initial energy. Instead, the photoelectric

effect describes the total absorption of the incident photon, causing the emission of an electron.

All these processes contribute to the total cross section (σ), which provides a measure of the photon-matter interaction probability. The contribution of each of the three interaction types reported above depends on the photons energy: above 1 MeV, the most probable processes are the pair production and the Thomson and Rayleigh scattering, while below this threshold the photoelectric effect is predominant.

1.1.2 Photoelectric effect

The main physical phenomenon behind the functioning of a photomultiplier tube is the photoelectric effect. Historically, it was first observed and reported in 1887 by Heinrich Hertz [1]. Since the wave nature of light couldn't agree with the experiments, a theoretical model explaining the experimental data was provided by Albert Einstein in 1905, using Max Planck's theory of light quantization and supporting the "particle nature" of light hypothesis. Einstein hypothesized that the light radiation is actually composed by discrete energy packets (which are known as "photons" today), each of them carrying a quantitative of energy E_γ proportional to the light frequency (ν) through the following equation:

$$E_\gamma = h\nu, \tag{1.1}$$

where $h = 6,62607015 \cdot 10^{-34}\text{J} \cdot \text{s}$ is the Planck's constant. For this reason, the light intensity depends on the number of photons which compose the light pulse.

The photoelectric effect consists of the absorption of a photon by an atom, causing the emission of one of its electrons, which is called "photoelectron". This phenomenon is also known as "photoemission". In order to observe this kind of process, the incident photon energy must be greater than the binding energy between the electron and the atom. During the process, the photon is completely absorbed (and thus the light intensity tends to decrease) and its energy is transmitted to the atom-electron system. If E_γ is sufficient to allow the electron to be emitted and ionize the atom, then (using Eq. (1.1)) the maximum electron kinetic energy (K) is subjected to the total energy conservation principle and is given by the following relation:

$$K = E_\gamma - B_E = h\nu - B_E \tag{1.2}$$

where h is the Planck's constant, ν is the light frequency and B_E is the electron binding energy. Therefore, Eq. (1.2) shows that there is a light threshold frequency ν_{th} below which there is no emitted photoelectron, since the impinging photon is not energetic enough. It can be computed by:

$$\nu_{th} = \frac{B_E}{h}. \tag{1.3}$$

Since the total momentum must be conserved, the absorption of the photon and the emission of a photoelectron cause the atom to recoil.

The photoelectric effect cross section σ_{photo} depends on the incident photon energy E_γ. In particular, it presents some peaks when E_γ equals the binding energy of the electron (*i.e.* the energy of the shells K, L, M etc.). This behaviour is shown in Fig. 1.1 in the case of lead, having a K absorption edge of about 88 keV. Around the peaks and at high energies (above 1 MeV) σ_{photo} decreases rapidly, and thus the photoelectric effect becomes less probable.

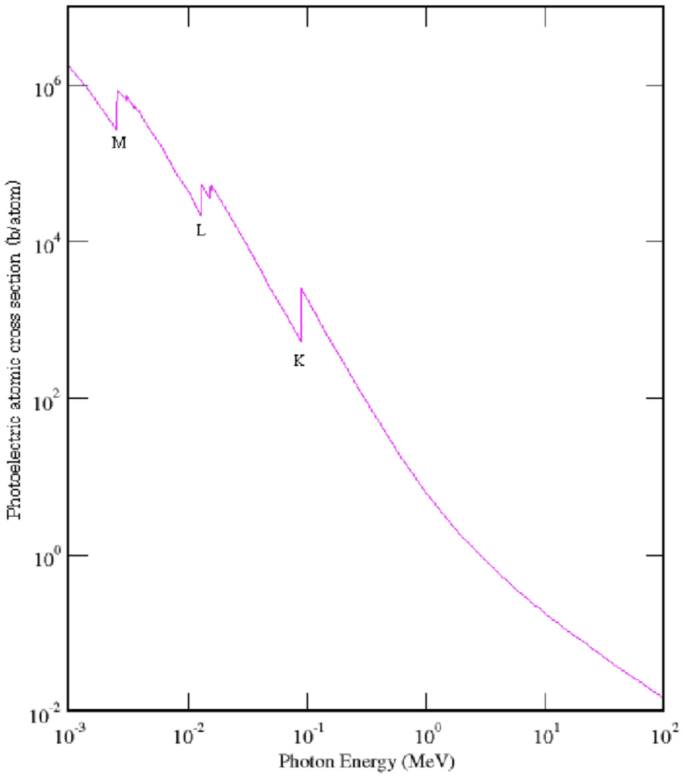

Figure 1.1: Photoelectric effect cross section of lead as a function of the incident radiation energy. The peaks in correspondence of K, L and M shells can be seen. The K absorption edge is at about 88 keV. Data from NIST [3].

1.2 Structure of a PMT

Photomultiplier tubes are vacuum glass tubes which can reveal the presence of photons thanks to the photoelectric effect. Their main purpose is to convert photons into photoelectrons, generating a current signal.

When a photon impinges on the so-called PMT window, a photoelectron can be emitted from the photocathode, which is the component just after the window. The flux of photoelectrons is focused by an electrode. Since the number of electrons produced by a single light pulse is too small to create a significant and detectable current signal, every PMT contains some amplification stages (*i.e.* the dynodes, called collectively as "dynode system"), which increases the number of electrons composing the current in order to amplify the output signal. The electrons are finally collected in the last electrode of the dynode system (the PMT anode), which outputs the produced current to an external circuit, allowing the signal to be acquired. A synthetic scheme of a typical photomultiplier tube structure is shown in Fig. 1.2.

The vacuum condition inside the PMT is necessary in order to facilitate the multiplication of the electrons in the dynode system, since the presence of any residual gas

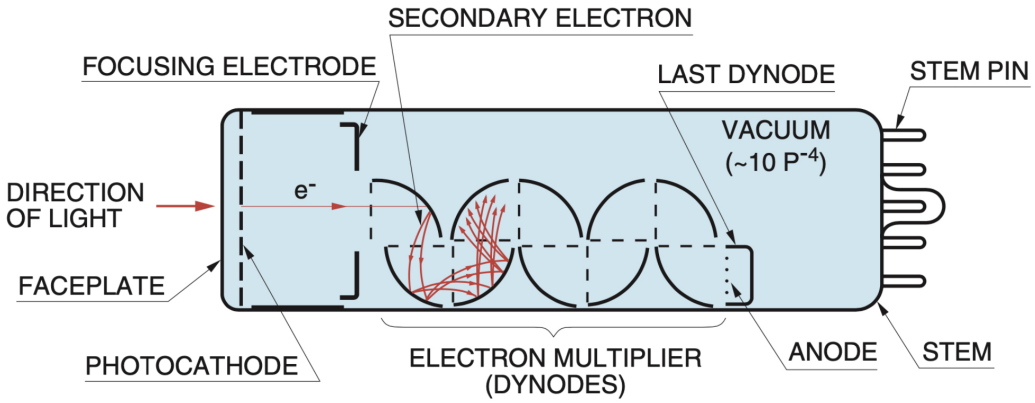

Figure 1.2: Synthetic scheme of the structure of a photomultiplier tube [1].

would cause the deceleration of the incoming ones. The glass tube allows the PMT to support the pressure gradient between the inner vacuum and the outer ambient.

1.2.1 Photocathode

The photocathode is the component of the PMT where the photoelectric effect takes place, and thus where the photoelectrons are emitted from the surface into the vacuum. It is placed just after the PMT window.

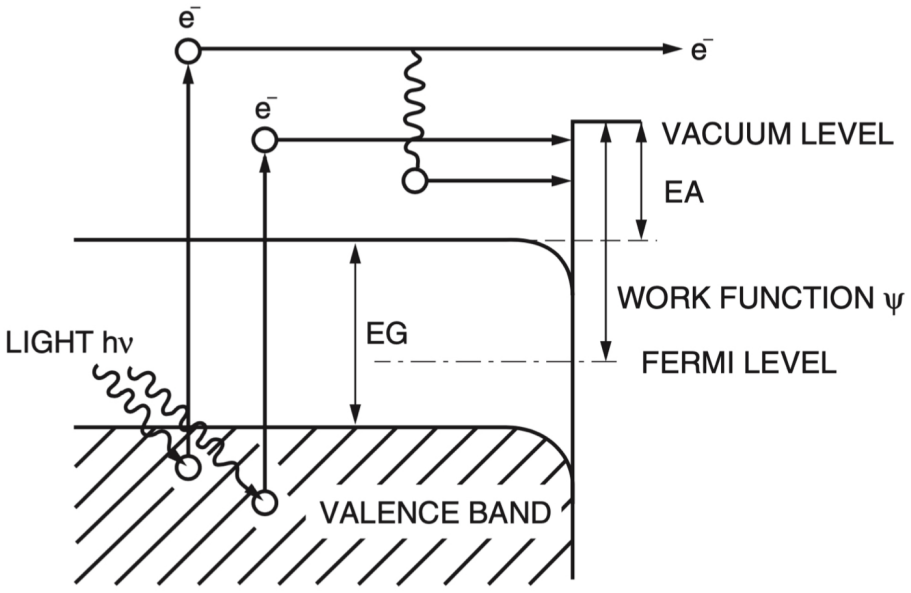

Figure 1.3: Illustration of the band model for a semiconductor material composing a photocathode. EA is the electron affinity, EG is the energy gap between the valence band and the conduction band, while the "work function" Ψ is defined as the energy difference between the vacuum level and the Fermi level of the semiconductor [1].

The material composing the photocathode is a semiconductor, which can be physically described by the band model. In this model, there are two main energy bands in which the electrons of the material can stay. The lower one is called "valence band" and above it there is a forbidden energy gap, which in normal conditions cannot be occupied by the electrons. At higher energies, there is the "conduction band", which can be occupied by electrons having enough energy to overcome the forbidden gap. If the incident photon is energetic enough to observe the photoelectric effect, an electron in the valence band can acquire sufficient energy to overcome the vacuum level barrier and thus to be emitted from the photocathode surface. The difference of energy between the vacuum level and the minimum of the conduction band is called "electron affinity" (EA). This model is illustrated in Fig. 1.3.

An important physical parameter describing the photocathode material interaction with radiation is the "quantum efficiency" (QE), which contains the information about the probability of the photon conversion into a photoelectron (*i.e.* the conversion efficiency) and the process dependence on the impinging radiation wavelength. It will be described in more detail later in this chapter.

1.2.2 Dynode system

The photoelectrons emitted from the PMT photocathode surface for a single light pulse are too few to create a detectable current signal. Therefore, PMTs contain a series of amplification stages, called dynodes, composed by electrodes which can increase the number of electrons and thus the intensity of the current signal. The structure of the dynode system can be different for various types of PMTs, in order to optimize the amplification.

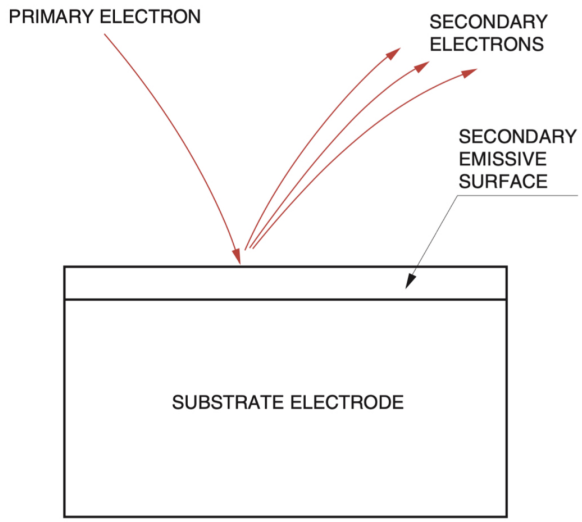

Figure 1.4: Illustration of the secondary emission process which takes place in the dynode system [1].

The electrons coming from the photocathode surface are accelerated by a potential difference and hit the first electrode, which is typically covered by a thin layer of sec-

ondary emissive material. The kinetic energy of the primary electrons is deposited in such layer, which is now excited and energetically allowed to emit secondary electrons, amplifying the initial current. By establishing a potential difference between each electrode, the same process is repeated until the electrons reach the PMT anode. Actually, not all the secondary emission electrons have the right direction and enough energy to hit the successive dynode stage and continue the multiplication process. A scheme of the secondary emission process is illustrated in Fig. 1.4.

The energy required to release the secondary electrons in the vacuum is usually between 2 eV and 3 eV, while the energy of the initial photoelectrons is typically about 1 eV (and thus a potential difference between the PMT cathode and anode is required). The different voltages of the amplification stages are provided by a "divider circuit": an external circuit having resistances which cause a voltage drop in correspondence of the dynodes.

1.3 The Hamamatsu R760 PMT

The PMT under study in the ageing campaign described in this thesis is a Hamamatsu R760 photomultiplier tube [4]. In this section, its main features are briefly presented.

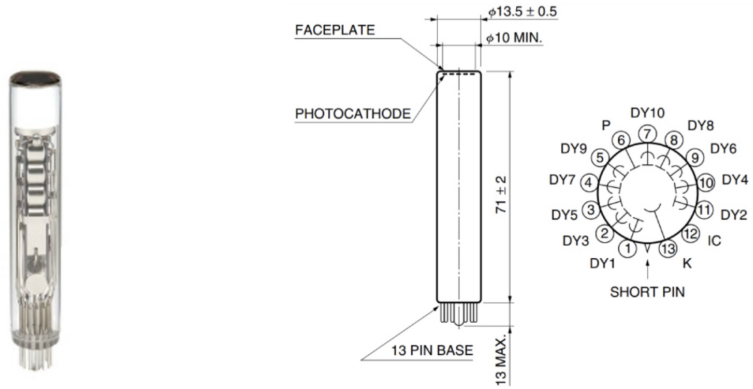

Figure 1.5: (Left) Picture of the R760 PMT and (right) its dimensional scheme.

The window of the R760 PMT is made of quartz and has a thickness of 1.2 mm, while its photocathode has a diameter of about 10 mm. It is a "head-on" type PMT, which means that the sensitive area is only on the top of the device. The photocathode is composed by a bialkali material, sensitive in the range between visible and ultraviolet light. In Fig. 1.5 a picture of this PMT (on the left) and its dimensional characteristics (on the right) are shown.

The PMT under study is sensitive to impinging photons with wavelengths in the range between 160 nm and 650 nm. In particular, its quantum efficiency (QE) exceeds the 15% from 200 nm to 500 nm, reaching the maximum value $QE_{max} \simeq 27\%$ at about 400 nm. These properties can be seen in Fig. 1.6, where the quantum efficiency and the photocathode radiant sensitivity (which will be defined and described more in detail in Sec. 1.4) of a R760 PMT as functions of the incident radiation wavelength are shown.

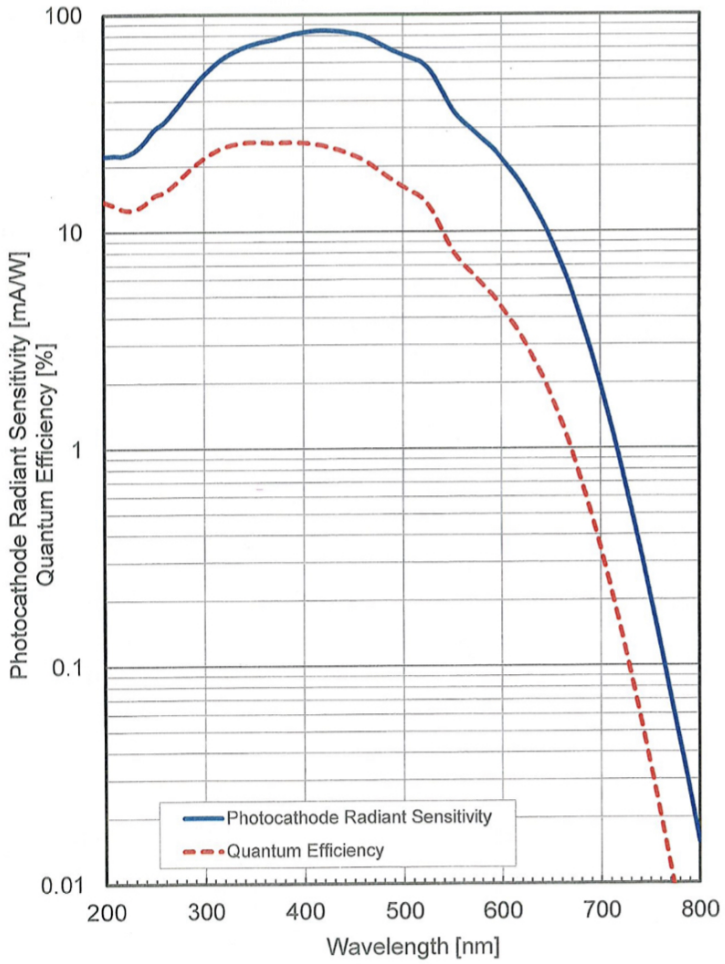

Figure 1.6: Quantum efficiency (red line) and photocathode radiant sensitivity (blue line) of a photomultiplier tube R760 as functions of the radiation wavelength, measured by Hamamatsu [2].

Its dynode system is composed by ten amplification stages. The divider circuit of the PMT under study provides eleven equal resistances placed between the photocathode and the anode, in order to reach the same voltage difference ΔV between every electrode of the dynode system. The circuit is in anode grounding. A scheme of this divider circuit, built at IJCLab, is shown in Fig. 1.7.

The voltage differences ΔV can be obtained by:

$$\Delta V = \frac{V}{n+1}, \tag{1.4}$$

where V is the alimenting voltage between the PMT photocathode and the anode, while $n = 10$ is the number of amplification stages. The denominator $n+1 = 11$ is the number of resistors, which can be obtained by looking at the structure of the divider circuit in Fig. 1.7. This particular relation will be used in Sec 4.2 in order to study the dependence between the gain and the applied high voltage.

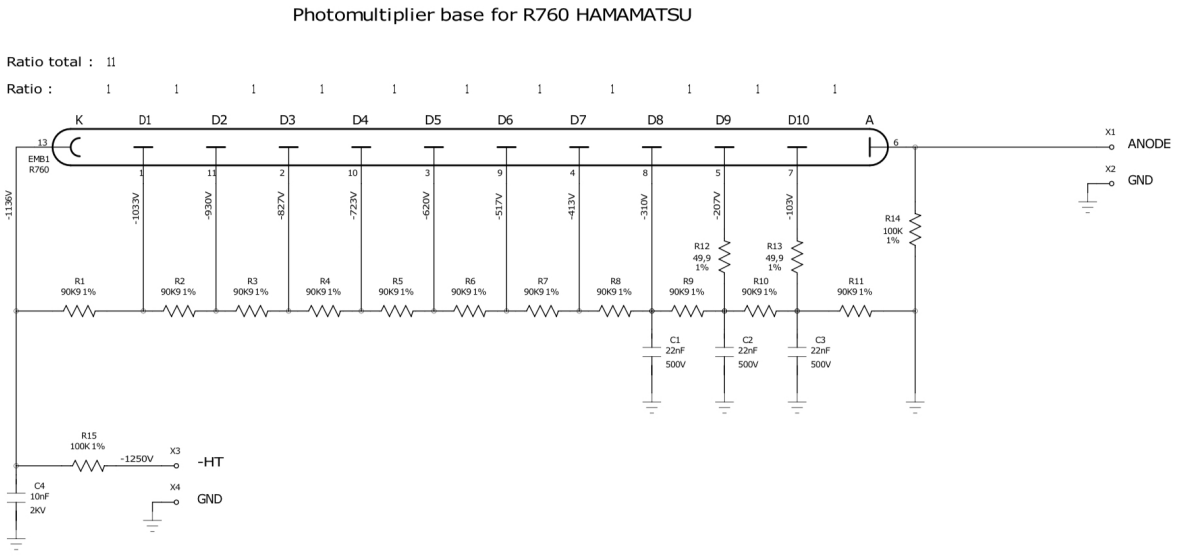

Figure 1.7: Scheme of the divider circuit of the R760 PMT under study, which was built at IJCLab [5].

1.4 Quantum efficiency

When photons impinge the PMT window, electrons in the valence band of the photocathode absorb their energy, become excited and start to diffuse towards the photocathode surface. If they have enough energy, they can be emitted into the vacuum as photoelectrons. This process has a probabilistic nature and is described by the "quantum efficiency" (QE) parameter, defined as the ratio between the number of incident photons and the number of produced photoelectrons. It is a function of the incident radiation's wavelength (λ) and can be expressed as [1]:

$$QE(\lambda) = (1 - R) \cdot \frac{P_\lambda}{k} \cdot \left(\frac{1}{1 + \frac{1}{kL}}\right) \cdot P_s, \tag{1.5}$$

where the parameters are:

- R: reflection coefficient of the photocathode material;
- k: full absorption coefficient of photons;
- P_λ: probability of the electrons to acquire enough energy to overcome the vacuum level barrier due to light absorption, at a fixed value of the radiation wavelength λ;
- L: mean escape length of excited electrons;
- P_s: probability of electrons to be released into vacuum when they reach the photocathode surface.

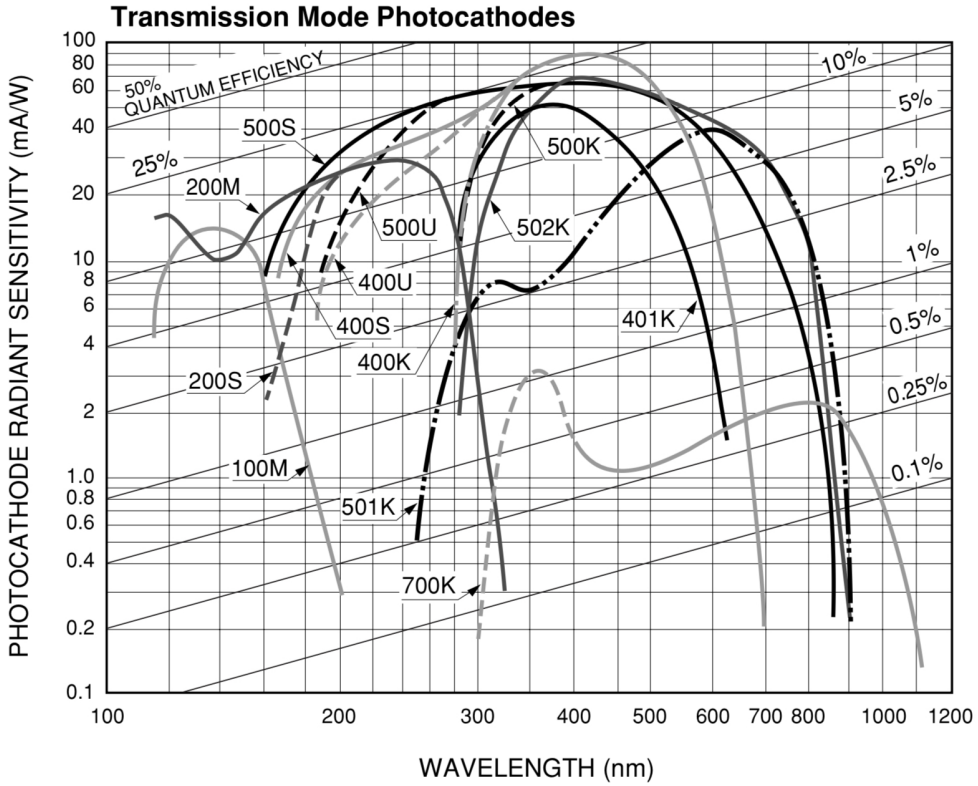

Figure 1.8: Typical radiant sensitivity behaviour as a function of the incoming radiation wavelength λ for different photocathode materials, also indicating the quantum efficiency values. The notation is the same used in [1]. In particular, 400S, 400U and 400K refer to bialkali photocathodes.

Since R, k and P_λ are constant for a chosen material (and a fixed incoming wavelength λ), the QE strongly depends on L, which can be increased by using better crystals, and P_s, which main dependence is on the electron affinity.

The dependence between QE and λ can be made explicit by defining the radiant sensitivity S_k of the PMT as the ratio between the photocurrent (I_{photo}) and the incident radiant flux (Φ_λ) at a fixed wavelength:

$$S_k = \frac{I_{photo}}{\Phi_\lambda}. \tag{1.6}$$

Therefore, the quantum efficiency as a function of λ, expressed in percent, can be expressed as:

$$QE(\lambda) = \frac{hc}{\lambda e} \cdot S_k \tag{1.7}$$

where h, c and e are the Planck's constant, the speed of light and the absolute value of the electron charge, respectively.

An example of typical radiant sensitivity behaviours at different radiation wavelengths is shown in Fig. 1.8 for different photocathode materials. All the graphs are below the $QE = 50\%$ line, reaching maximum values around $QE \simeq 25\%$.

1.5 Gain

One of the most important operational characteristics of a PMT is the gain (G). It measures the ability of the dynode system to amplify the signal and it is defined as the ratio between the anode current I_{anode} and the initial photocathode current I_0:

$$G = \frac{I_{anode}}{I_0}. \tag{1.8}$$

Since the latter isn't accessible in general, a way to obtain the PMT gain is to reach the "single photoelectron" condition (S.P.E.), consisting of having only one photoelectron emitted from the photocathode surface for every light pulse hitting the PMT window. The S.P.E. condition will be described in detail later in this thesis, in Sec. 3.1.

The process of current amplification performed by each dynode has a statistical nature. The amplification factor (δ) of a single dynode provides the expected number of secondary emitted electrons ($N_{secondary}$), given the number of the incident ones ($N_{incident}$):

$$\delta = \frac{N_{secondary}}{N_{incident}}. \tag{1.9}$$

The emission of secondary electrons depends on the energy transmitted by the incident ones, accelerated by the voltage difference between the dynodes (ΔV). Thus, δ is a function of ΔV and it is expected to follow a power law:

$$\delta = C \cdot \Delta V^k, \tag{1.10}$$

where k depends on the structure and material composing the dynodes and C is a constant. By taking the definition of δ, the amplification factor of each dynode can be written as the ratio between the emitted current I_n and the incident current I_{n-1}, where n labels the dynode:

$$\delta_n = \frac{I_n}{I_{n-1}}. \tag{1.11}$$

When a secondary electron is emitted, it could deviate from its favorable trajectory, missing the successive dynode and not taking part in the current amplification process. Since the number of electrons increases greatly in the dynode system, the main contribute of this type is given by the first photoelectron. The probability that the latter hits the first dynode's emissive layer is called "collection efficiency" (later indicated as α_{eff}). Typically, it grows as the the voltage difference between the photocathode and the first dynode increases. Therefore, considering a dynode system composed by N amplification stages, the anode current can be obtained by the relation:

$$I_{anode} = I_0 \cdot \alpha_{eff} \cdot \prod_{n=1}^{N} \delta_n, \tag{1.12}$$

leading to the following equation for the PMT gain:

$$G = \alpha_{eff} \cdot \prod_{n=1}^{N} \delta_n. \tag{1.13}$$

If we consider a PMT having a high collection efficiency ($\alpha_{eff} \simeq 1$) and the same voltage difference ΔV between all the dynodes (such as the R760 PMT under study in this ageing campaign), the gain as a function of ΔV follows the relation:

$$G = \delta^n = (C \cdot \Delta V^k)^n, \tag{1.14}$$

where δ is assumed to be the same for every amplification stage and constant.

Therefore, under the same operating conditions (for example, under the S.P.E. condition), the output current signals would have the same amplitude. In practice, since δ describes a statistical phenomenon, it varies around a mean value and thus the output signals are subjected to statistical fluctuations.

In the case of the R760 PMT under study having the divider circuit illustrated in Fig. 1.7, by using (1.14), the gain as a function of the voltage V between the photocathode and the anode can be written as:

$$G = \left(C \cdot \frac{V^k}{(n+1)^k}\right)^n \tag{1.15}$$

where $n = 10$ is the number of amplification stages. Then, by defining $A = C^n/(n+1)^{kn}$ and $\alpha = k \cdot n$, Eq. (1.15) becomes:

$$G = A \cdot V^\alpha \tag{1.16}$$

which shows the explicit power law connecting the gain and the high voltage between the PMT photocathode and the anode.

Due to the presence of the resistors R14 and R15 in the divider circuit illustrated in Fig. 1.7, the high voltage V_a alimenting the PMT is different from V. In particular, they follow the relation:

$$V \simeq \frac{V_a}{1.1}. \tag{1.17}$$

Thus, since V can be obtained by rescaling V_a through Eq. (1.17), the dependence between the PMT gain G and V_a is a power law of the same type of Eq. (1.16). Later in this document, the indicated voltages will always refer to the alimenting voltages V_a, if not explicitly specified.

1.6 Ageing of a PMT

When a photomultiplier tube powered on is exposed to a source of light or to a high particle rate for long periods of time, it is affected by a variation of some of its operational characteristics. The process of deterioration of its nominal performances is called "ageing" of the PMT. In general, it depends on the previous operating history, the dynodes materials and the output current levels of the PMT and it brings to an overall sensitivity and gain decrease.

The ageing process physical description involves three main aspects [6]:

- wear of the dynode system;
- increase of the dark current;

- decrease of the photocathode efficiency.

The first one is probably caused by the erosion of the dynodes surfaces (when they are being hit by significant electrons fluxes), with a subsequent deposition of the dynodes materials in other regions of the photomultiplier [7]. Therefore, since the PMT gain depends on the amplification process performed by the dynodes (as explained in the previous section), the output signal current tends to decrease, as the dynodes wear out. The overall consequence consists in a decrease of the PMT gain.

The dark current is a typically small current generated in the PMT by noise sources. It circulates even when there is no light impinging the PMT window. Thus, it contributes in the output current signal as noise and it tends to increase during the aging process.

The loss of photocathode efficiency affects the capability of the PMT to detect incident photons. Therefore, as the ageing goes on, an increasing number of photons impinging the PMT window doesn't produce any photoelectron via the photoelectric effect, remaining undetected.

In some cases, the process of ageing can be reversed by having the PMT undergo non-operation periods of time. Such recovery periods may be able to provoke an increase of the PMT gain and overall sensibility to light pulses. This possibility has been studied in the work documented in this thesis by switching off the PMT for 20 days during the ageing process and resuming it afterwards.

Chapter 2

Experimental setup and campaign structure

In this Chapter, the experimental procedures used to study the gain and the ageing of the Hamamatsu R760 photomultiplier are explained. Firstly, the experimental setup is shown. Then, the length and time structure of the ageing campaign will be discussed.

2.1 Experimental setup

The source of light impinging the PMT window was a Thorlabs LED [8], having a wavelength peaking at 525 nm. The PMT has been installed on a support facing the LED. Both the LED and the PMT were placed inside a dark box, which did not allow any light coming from the outside to impinge the PMT window and produce noise spurious signals.

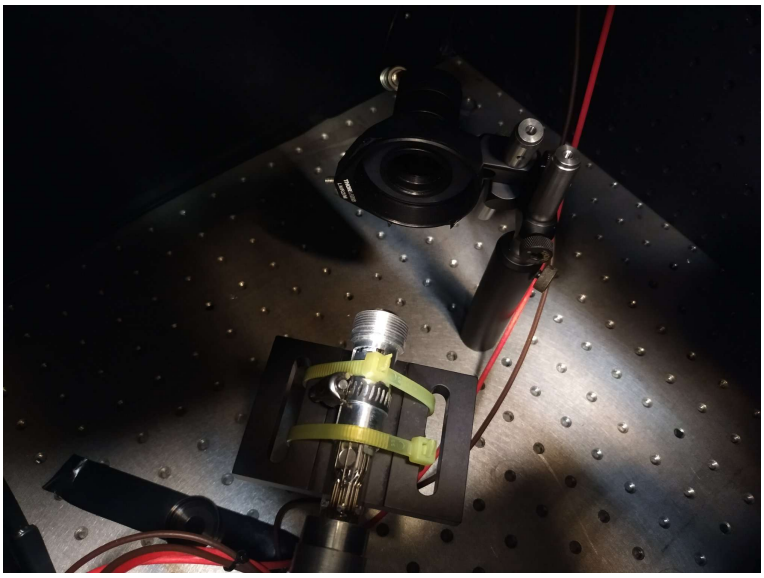

Figure 2.1: A picture of the inside of the dark box in which the LED and the PMT under study were placed.

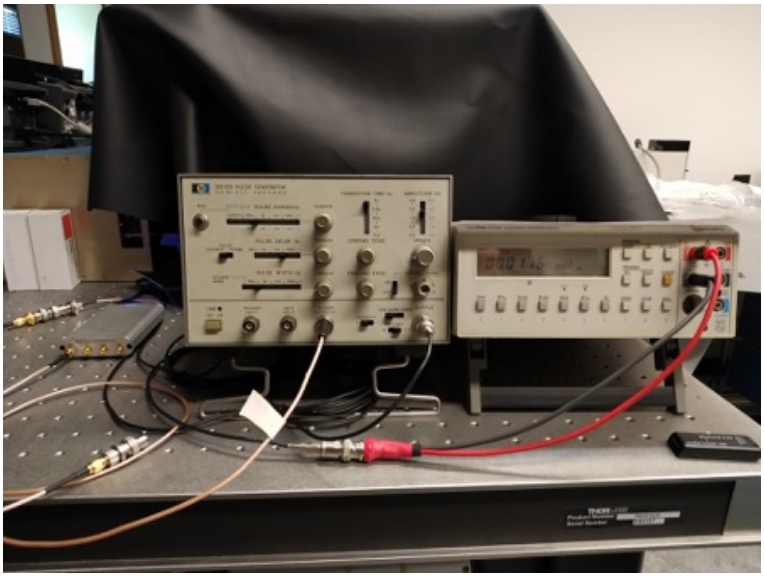

Figure 2.2: From left to right: the DRS4 Evaluation Board, the HP-8012B pulse generator and the Philips 2534 System Multimeter used in the ageing campaign. Behind them the external part of the dark box can be seen.

A picture of the inside of the dark box is shown in Fig. 2.1, where the PMT under test and the LED can be seen.

During the ageing, the LED was operated in an approximately continuous wave regime, with a pulse frequency of 50 MHz and a 20 ns pulse width. To measure the absolute gain, the LED was then switched to a pulsed regime, with a frequency of 500 Hz and a greater voltage bias in order to achieve the S.P.E. condition. Finally, in order to realize the "relative method" measurements (described in Sec. 3.3), the LED was again operated in an approximately continuous wave regime. The LED voltage and pulse frequency have been set by using a HP-8012B pulse generator [9].

The power supply was provided by a 40 Channel High Voltage System SY127 from CAEN [10]. During the ageing, the PMT supply voltage was set to 1200 V, while for the absolute gain measurements (described in Sec. 3.2) it was set to 1375 V, reaching a value of 1250 V between the PMT photocathode and the anode.

In order to monitor the anodic current and to perform the relative gain measurements, a Philips 2534 System Multimeter [11] has been used, having a resolution of 100 nA. To measure the absolute gain, the PMT signal was acquired and digitized by a DRS4 Evaluation Board provided by Paul Sherrer Institute (PSI) [12] in the channel 1 (during the first three measurements sessions) or 2 (for all the other data acquisitions), thanks to a trigger signal coming from the HP-8012B pulse generator. A picture of the DRS4 Evaluation Board, the HP-8012B pulse generator and the Philips 2534 System Multimeter is shown in Fig. 2.2, while a synthetic scheme of the experimental setup is illustrated in Fig. 2.3.

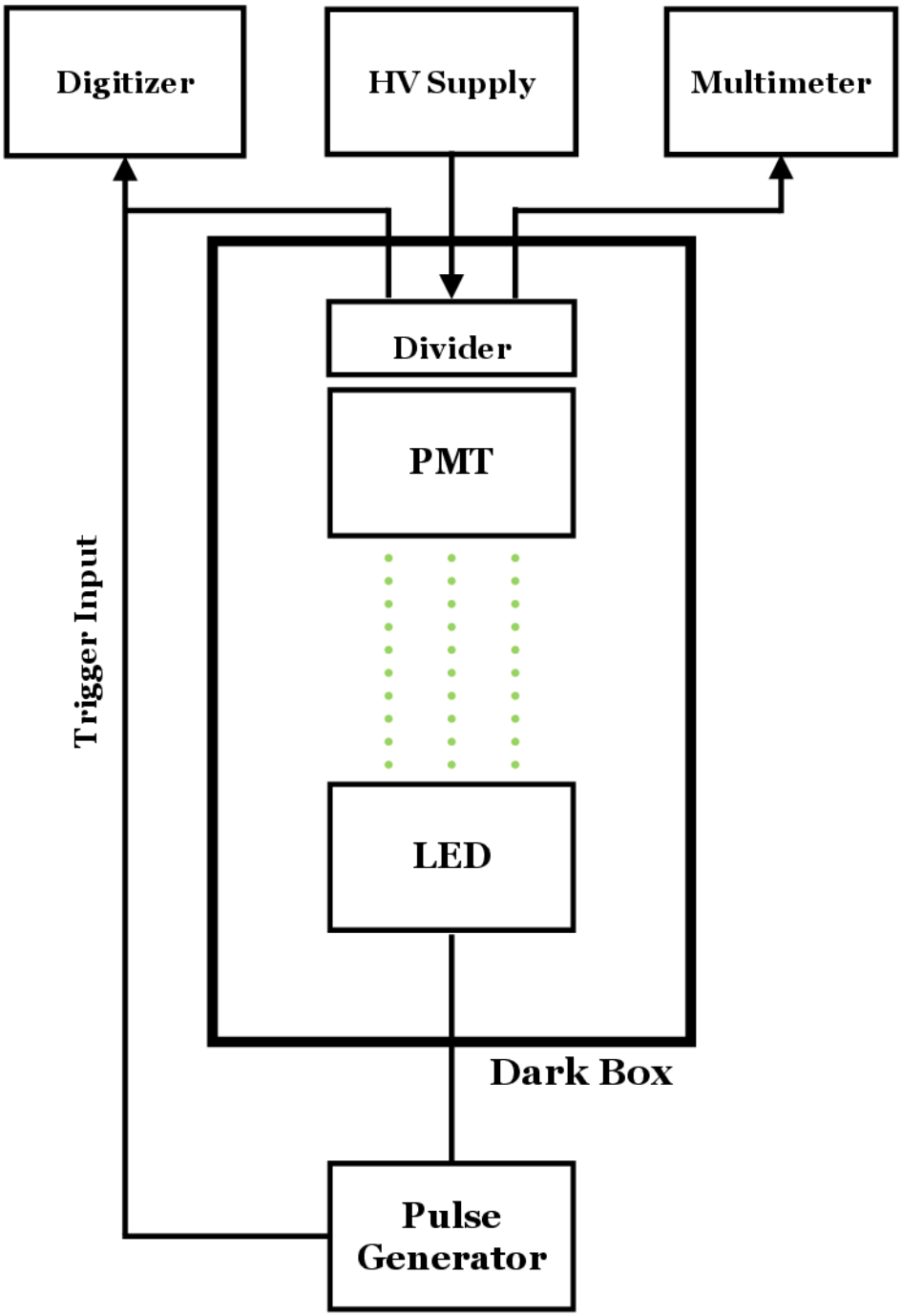

Figure 2.3: A scheme of the experimental setup used during the ageing campaign.

2.2 Ageing campaign structure

The whole ageing has been monitored by measuring the PMT anode current, using the Philips 2534 System Multimeter. From the current measurements, it has been possible to obtain the integrated charge as a function of the ageing time through a numerical integration. All the measurements have been performed between the dates 10/22/2021

and 01/21/2022. The ageing campaign was divided into three main parts: a first ageing period from 10/22/2021 to 12/21/2021, followed by a recovery one from 12/21/2021 to 01/10/2022, and finally a second ageing period between 01/10/2022 and 01/21/2022.

First, the PMT under study has been submitted to the LED light at a fixed voltage of 1200 V for 60 days, achieving an integrated charge of about 282 C. Then, the ageing has been stopped for 20 days in order to study a possible increase of the PMT gain after a recovery period. Finally, the ageing was resumed for 10 days, reaching a total integrated charge equal to 342 C. This can be seen in Fig. 2.4, where the values of current produced by the PMT (a) and integrated charge (b) as function of the days of ageing are shown. The recovery period (between the 60th and 80th day of ageing) is indeed characterized by a null current and a constant value of integrated charge. The value of integrated charge collected corresponds to roughly 5 years of LHCb data taking with Run 3 conditions, well over the foreseen lengeth of Run 3, scheduled to end by 2025.

The peaks in Fig. 2.4 (a) correspond to the measurements sessions: in order to perform the relative gain measurements discussed in Sec. 3.3, the LED bias had to be increased to achieve a current of about 100 μA at maximum PMT voltage. This last value has been chosen in order to make sure that all the measurements at decreasing high voltages (and current values) described in Sec. 3.3 could be performed. Due to a light blackout in the laboratory, the ageing accidentally stopped between the 14th and the 16th day, at an integrated charge value of about 60 C. Due to the PMT ageing and the consequent decrease of the gain, the current tended to diminish and thus, after every measurements session, the LED bias from the HP-8012B pulse generator had to be tuned to achieve a current between 50 μA and 100 μA.

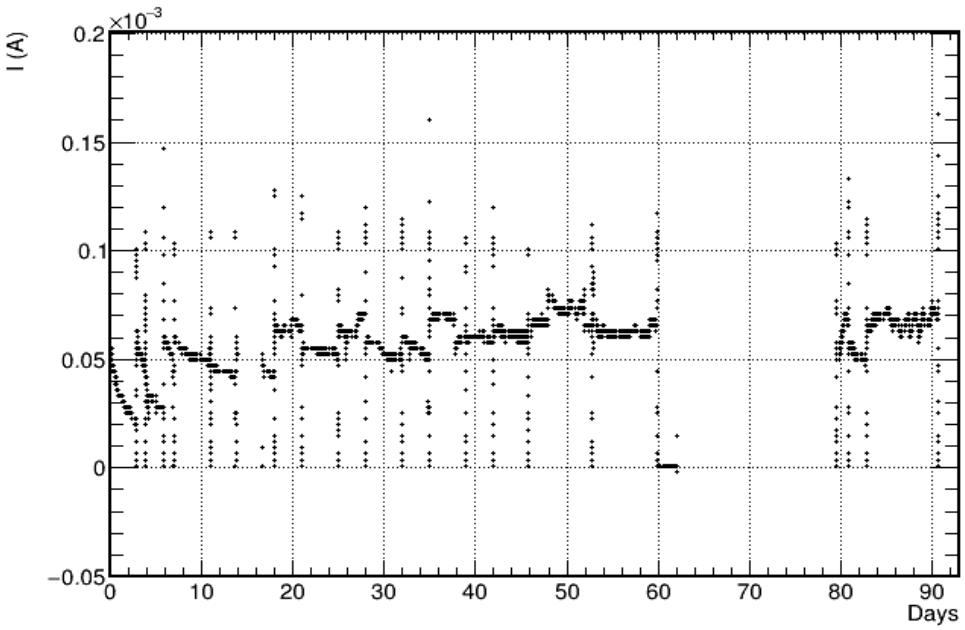

(a)

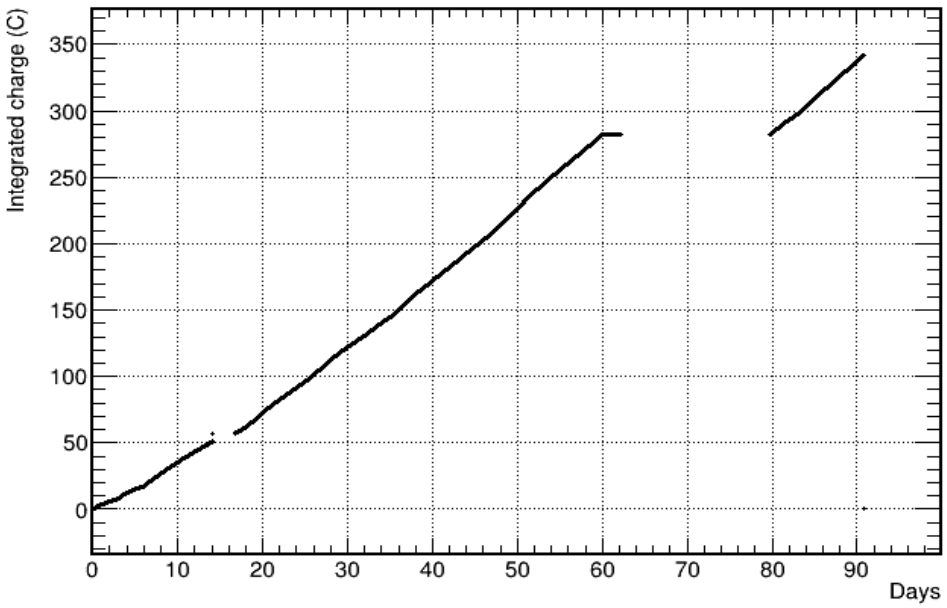

(b)

Figure 2.4: (Top) Anodic current from the PMT as a function of time, measured during the whole ageing campaign and (bottom) corresponding integrated charge. The gap between the 60th and 80th day corresponds to a recovery period, during which the PMT was turned off, while the one between the 14th and the 16th was caused by a light blackout in the laboratory.

Chapter 3

Gain measurements

In order to measure the PMT gain, two different methods have been employed. The first one ("absolute gain") consists of a single gain measurement, in which the gain value is obtained from a fit to the integrated-charge distribution of the PMT when operated in the single photoelectron (S.P.E.) mode, described in detail in the first section of this Chapter. The second one ("relative gain") employs a different approach in order to study the gain behaviour at different voltages. These approaches will be discussed in detail in the next sections.

3.1 Single photoelectron condition

As described in Sec. 1.5, the PMT absolute gain is defined as the ratio between the anode current and the photocatode current. The latter is generated by the photoelectric effect when photons hit the PMT window and since in general it is not accessible, the absolute gain cannot be directly measured in this way. The strategy to overcome this problem is to reach the S.P.E. condition, which consists of having only one photoelectron emitted from the photocathode for every light pulse hitting the PMT window. In this case, the photocathode current is composed only by a single photoelectron charge ($e = -1.6 \cdot 10^{-19}$ C), which is then amplified by the PMT dynode system. Thus, the absolute gain can be obtained by measuring the total charge of the PMT signal.

The number of photons hitting the PMT window in general follows a Poisson distribution. Since both the conversion of the incident photon into a photoelectron (by the photoelectric effect) and the collection of electrons by the dynode system are random binary processes, the number of photoelectrons producing a PMT signal is still described by a Poisson distribution. Thus, the number of detected events (N_k) follows the equation:

$$\frac{N_k}{N_{tot}} = \frac{\nu^k}{k!} \cdot e^{-\nu}, \tag{3.1}$$

where k is the number of produced photoelectrons, ν represents the most probable value of the Poisson distribution and N_{tot} is the total number of events collected by the PMT, composing the PMT signal. In order to reach the S.P.E. condition, the probability of having events with no emitted photoelectrons has to be $P(k = 0) = N_0/N_{tot} \geq 0.95$, such that the number of events N_k with $k > 1$ is approximately zero. Thus, most of the events will be empty events, while the remaining part will be composed (almost) only

by events with only one photoelectron emitted ($k = 1$). By setting $k = 0$ in Eq.(3.1), ν must satisfy the condition:

$$\nu = -\ln\left(\frac{N_0}{N_{tot}}\right) \simeq -\ln(0.95) \simeq 0.05 \tag{3.2}$$

The value of ν can be obtained by measuring the rate of the null events N_0/N_{tot} using the digitizer. Therefore, before every absolute gain measurement, the rate of signal events is set to about 0.05 by varying the amplitude of the signal from the HP-8012B pulse generator alimenting the LED.

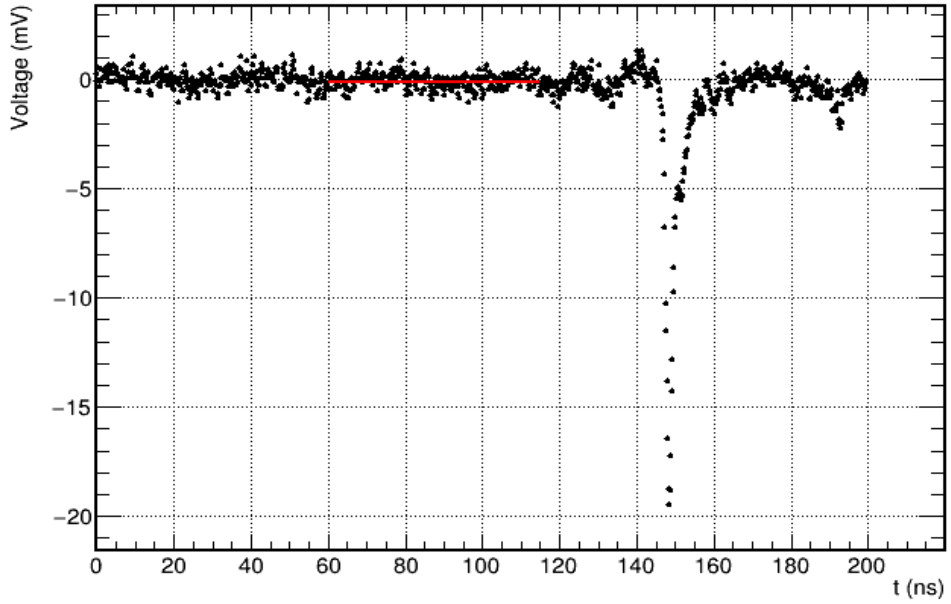

Figure 3.1: Example of the digitized PMT signal in S.P.E. condition. The horizontal red line overlaid is a linear fit in the region where no signal is present, thus giving an estimated baseline.

The rate of the null events (N_0/N_{tot}) has been obtained through the measurement of the number of events which exceeded the -5 mV threshold in the PMT signal acquired by the DRS4 Evaluation Board. This threshold has been chosen in order to avoid spurious counts due to the electronic noise of the DRS4 board. The quantity ν depends on the number of these events ($N_{<-5mV}$) by the following equation:

$$\nu = -ln(1 - R), \tag{3.3}$$

where $R = N_{<-5mV}/N_{tot}$. The value of R depends on the number of photons n_{ph} hitting the PMT window and the quantum efficiency (QE). Since the latter is constant for a fixed wavelength of the LED light, R (and therefore ν) can be varied acting on n_{ph}. For this reason, the right value of $\nu \simeq 0.05$ (and therefore the S.P.E. condition) has been reached by varying the amplitude of the signal from the HP-8012B pulse generator alimenting the LED.

An example of a digitized PMT signal in S.P.E. condition is shown in Fig. 3.1, with a horizontal linear fit overlaid. The fit has been performed in the a region where no signal is present in order to obtain the baseline of the PMT signal, which has been then subtructed from the measurements. Thus, systematic offsets regarding the measurement of ν have been corrected on an event by event basis.

3.2 Absolute gain

The absolute gain is measured at a fixed voltage of 1375 V once the S.P.E. condition described in the previous section is reached. By integrating the PMT pulse signal, the value of charge collected by the PMT anode is obtained. The integration time must be wide enough to contain a whole PMT signal. Thus, it has been chosen to be 40 ns. In order to subtract a possible offset in the PMT signal, horizontal linear fits in the region where no signal is present have been performed. An example of digitized PMT signal is shown in Fig. 3.1, where the linear fit overlaid shows the signal baseline.

From the distribution of the integrated charge, it is possible to estimate the gain from a fit by adapting a model to the data. This particular model has to consider the two main processes involved in the charge multiplication inside a PMT: the first one is a Poisson process related to the number of photoelectrons emitted by the quartz window (due to the photoelectric effect) and collected by the first dynode. The latter is due to the charge amplification process and the associated fluctuactions that occur at each dynode and it can be described by a Gaussian function. For these reasons, the fit model for the integrated charge distribution of the PMT in S.P.E. condition is given by the following equation:

$$\begin{aligned} M_{charge}(x) = N \Bigg[& \frac{\nu^0}{0!} e^{-\nu} \cdot \frac{1}{\sqrt{2\pi\sigma_p^2}} \exp\left(- \frac{(\mu_p - x)^2}{2\sigma_p^2} \right) \\ & + \sum_{n=1}^{5} \frac{\nu^n}{n!} e^{-\nu} \cdot \frac{1}{\sqrt{2\pi\sigma_g^2}} \exp\left(- \frac{(x - n\mu_g)^2}{2n\sigma_g^2} \right) \Bigg]. \end{aligned} \tag{3.4}$$

Here, the first term includes the product between the Poisson distribution with most probable value ν and a Gaussian distribution centered around zero, with mean $\mu_p \simeq 0$ and standard deviation σ_p. It describes the so called "pedestal" *i.e.* the events with no emitted photoelectrons, which are the majority due to the S.P.E. condition. Then, the second term contains a sum of products similar to the first one, with the number of produced photoelectrons varying between $1 \leq n \leq 5$. The mean of these last Gaussian distributions is set to n times the mean of the single photoelectron one. Despite the main term of the sum is the one with $n = 1$ thanks to the S.P.E. condition, there is a non-negligible amount of events with more than one photoelectron involved, which affects the measured gain value. The term N is a normalization constant.

In this model, the fraction of events in which the photoelectrons have skipped the first dynode stage, arriving directly to the second one and causing a lower amplification, has been ignored (its contribution is less important than the other terms).

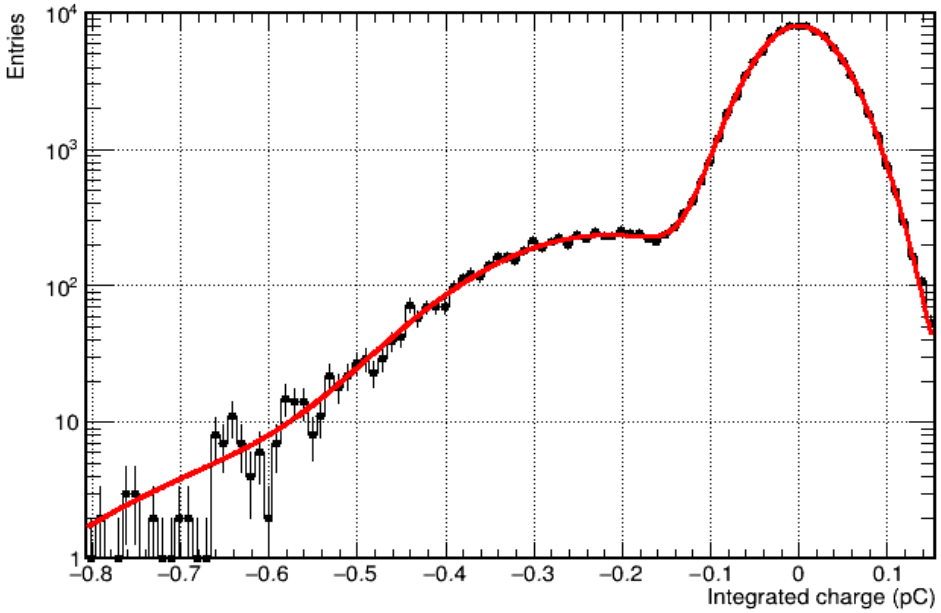

Figure 3.2: Example of a fit to the integrated-charge distribution, using Eq. (3.4), plotted in logarithmic scale. This measurement has been made during the 54th day of ageing, at about 245 C of integrated charge.

An example of a fit to the integrated-charge distribution using Eq. (3.4) is shown in Fig. 3.2.

The gain value can be obtained from the fit parameters through the relation:

$$G = \frac{\mu_g - \mu_p}{q_e} \cdot 10^{-12}, \tag{3.5}$$

where q_e represents the electron charge in Coulombs, μ_p is the mean value of the Gaussian p.d.f. describing empty events (*i.e.* the pedestal) and μ_g is the one concerning the events with only one emitted photoelectron. Since the mean of the pedestal μ_p is in general different from zero (due to electronic noise), the gain depends on the difference between μ_g and μ_p. The last factor 10^{-12} is a conversion constant.

3.2.1 Measurements

In Figs. 3.3, 3.4, 3.5, 3.6 and 3.7 the integrated-charge distributions obtained at different ageing steps are shown, with the results of the fits superimposed. For each integrated-charge point, around 100000 events have been acquired in order to have a sufficient amount of S.P.E. events. The peak around 0 pC, *i.e.* the pedestal, corresponds to the empty events described by the first term of Eq. (3.4). The width of this peak is caused by the noise of the electronics of the experimental setup. The other peak, whose position varies during the PMT ageing, represents the Gaussian distribution of the events with one emitted photoelectron (the events corresponding to the emission of more than one photoelectron are considerably less probable thanks to the S.P.E. condition). The PMT

absolute gain is obtained by measuring the difference of the averages of these two peaks, using Eq. (3.5). In fact, the PMT ageing can be noticed by looking at the decrease of this difference as the integrated charge grows. In the right part of Figs. 3.3, 3.4, 3.5, 3.6, and 3.7 the fits pull distributions are shown.

The pull distributions are calculated for each point of the integrated-charge distribution, by means of the following equation:

$$Pull(x_i) = \frac{x_i(fit) - x_i(data)}{\sigma_i(data)} \tag{3.6}$$

where where $x_i(fit)$ ($x_i(data)$) represents the value of the model (data point) in the i-th bin and $\sigma_i(data)$ is the uncertainty of the i-th bin. In order to have good compatibility between data and the fit model, there should not be visible accumulations above or below the x axis in the pull distribution graphs. This only occurs in the first three fits in Fig. 3.3. These sets of data have been collected using the 1st acquisition channel of the DRS4 Evaluation Board, while for the following measurements the 2nd one has been used. The reason for this discrepancy between the data and the fit model is most likely due to a miscalibration of the DRS4 Evaluation Board 1st aquisition channel, which caused a not perfectly Gaussian pedestal. However, fits in restricted ranges have been performed in order to check that the obtained gain values are correctly measured. Since all the checks provided gain values compatible within their uncertainties, systematic uncertainties haven't been added.

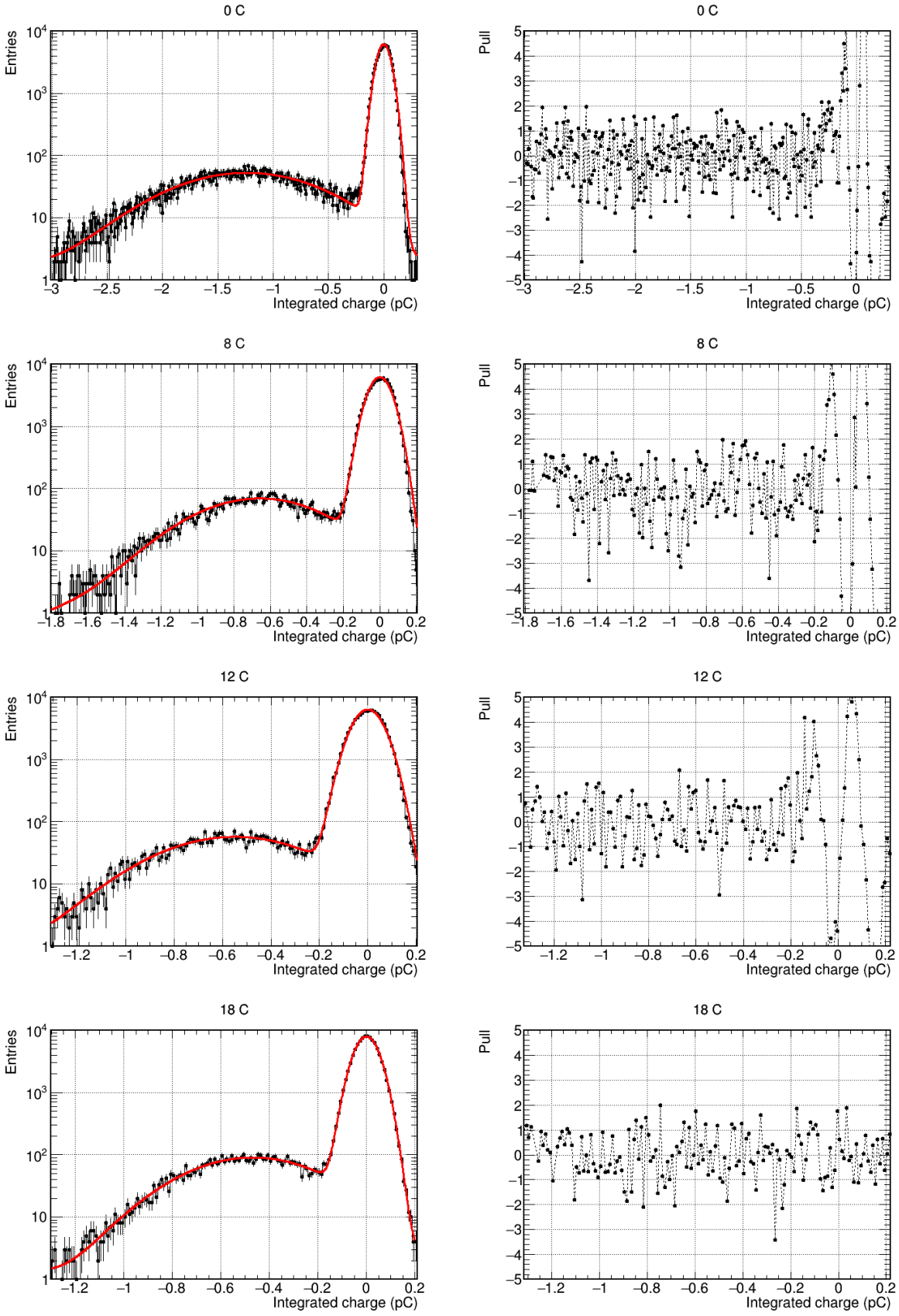

Figure 3.3: (Left) Integrated-charge distributions with the results of the fits overlaid and (right) corresponding pull distributions for (from top to bottom) different values of integrated charge.

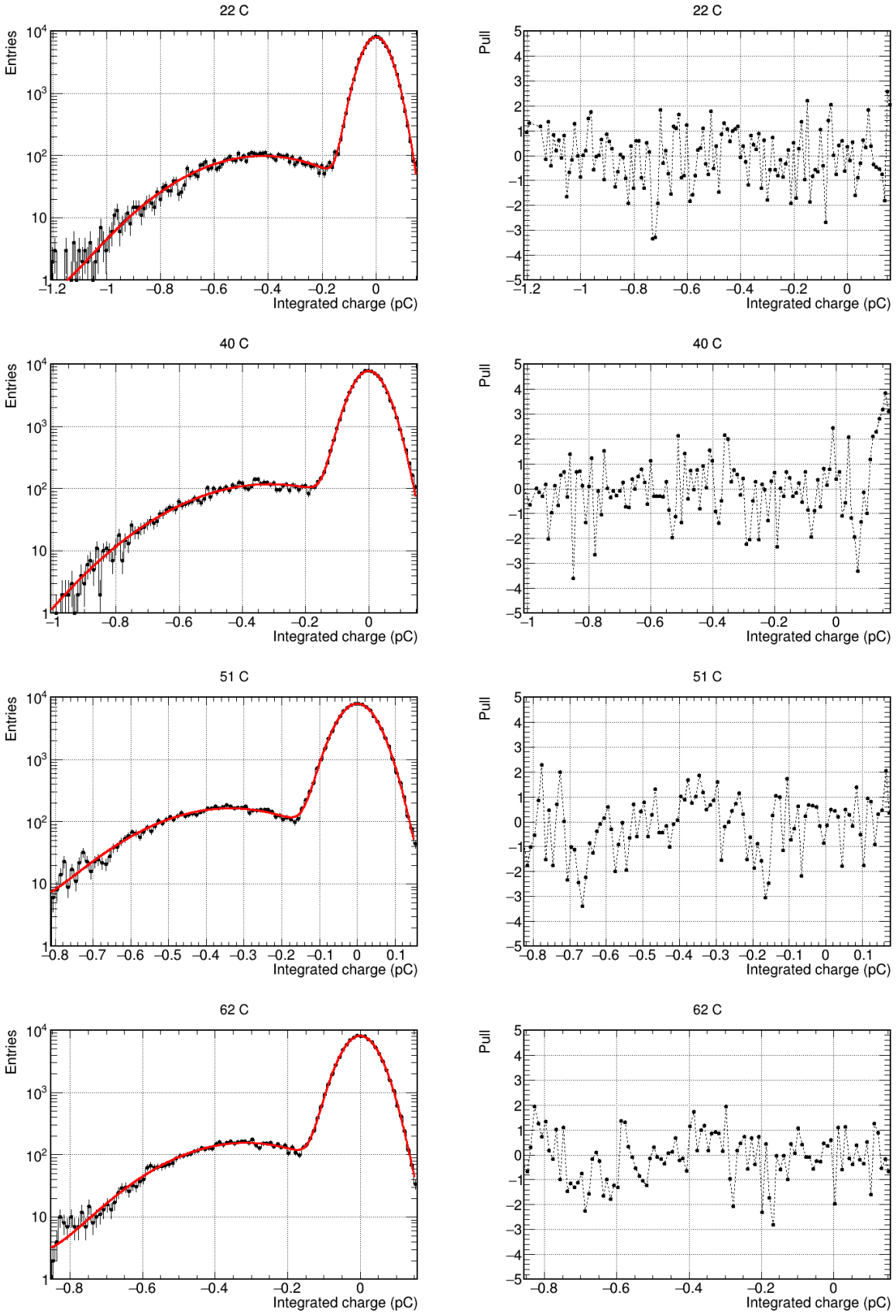

Figure 3.4: (Left) Integrated-charge distributions with the results of the fits overlaid and (right) corresponding pull distributions for (from top to bottom) different values of integrated charge.

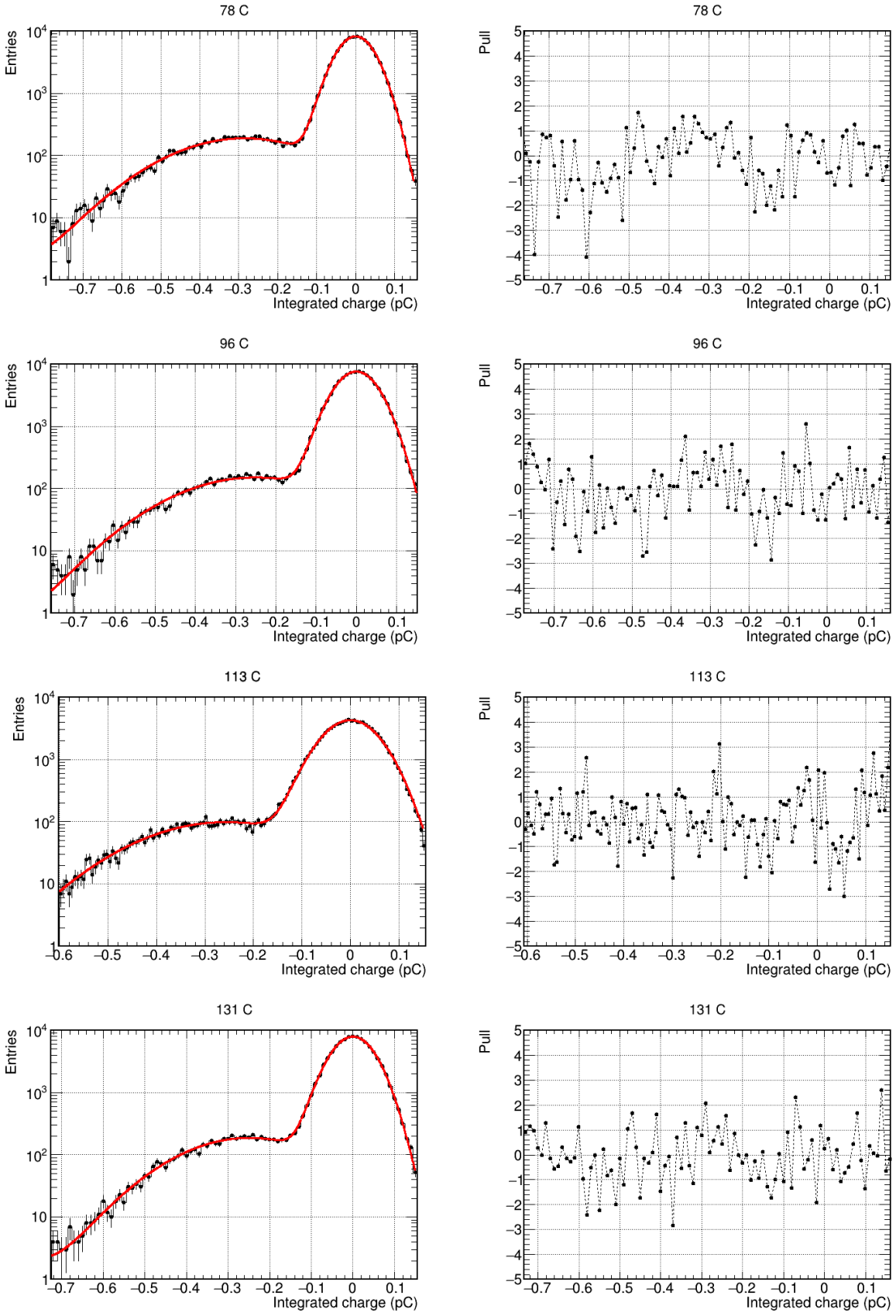

Figure 3.5: (Left) Integrated-charge distributions with the results of the fits overlaid and (right) corresponding pull distributions for (from top to bottom) different values of integrated charge.

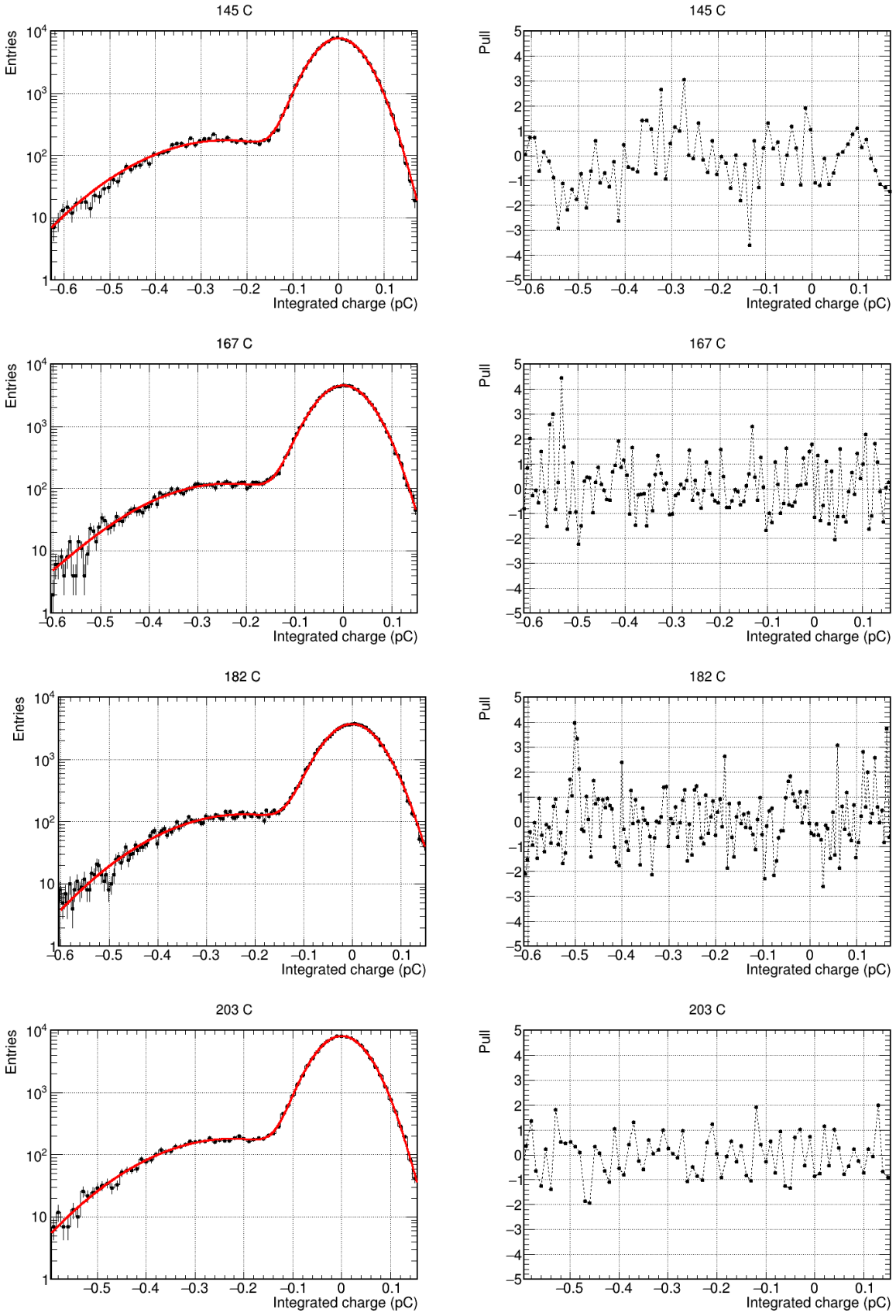

Figure 3.6: (Left) Integrated-charge distributions with the results of the fits overlaid and (right) corresponding pull distributions for (from top to bottom) different values of integrated charge.

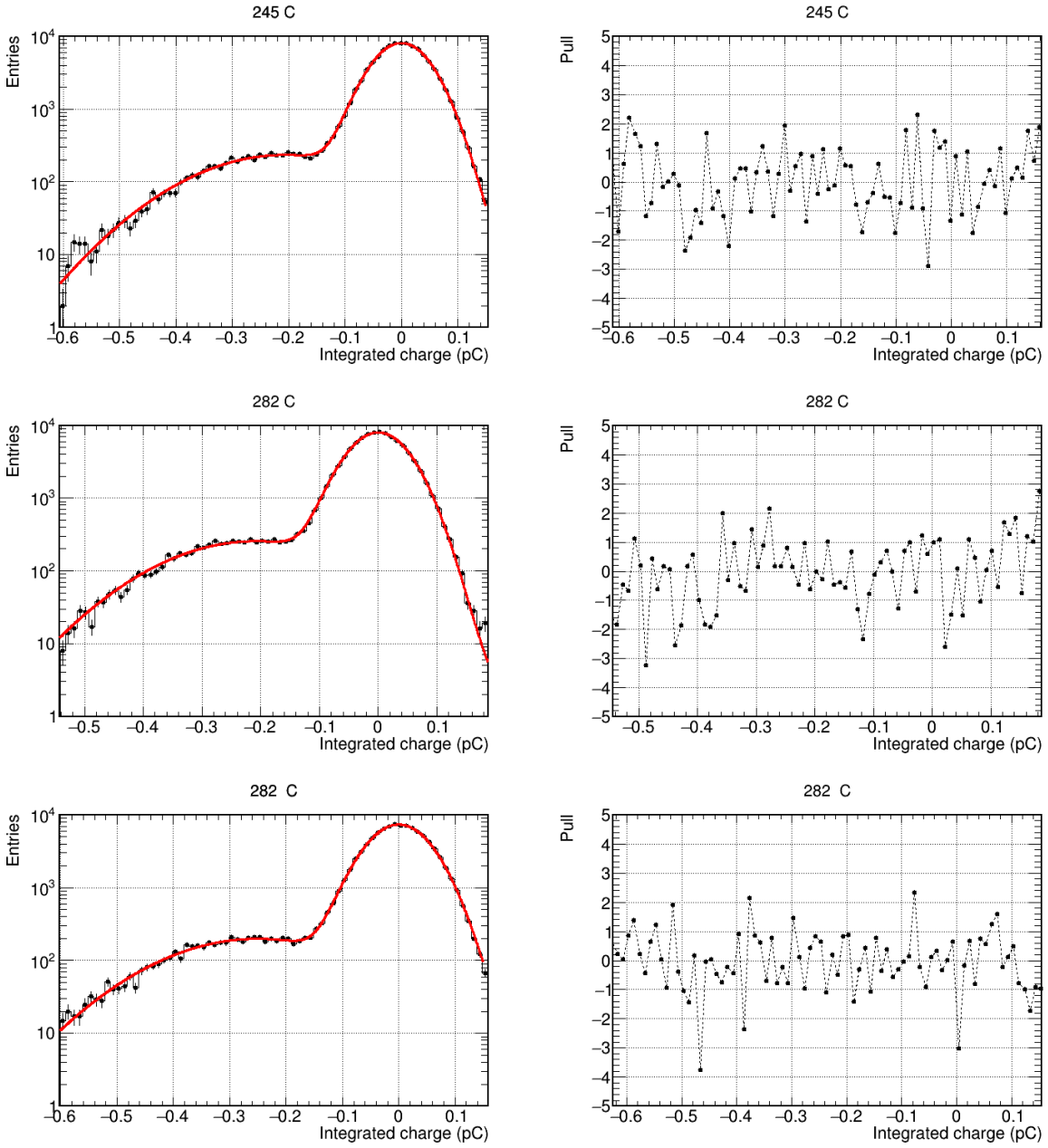

Figure 3.7: (Left) Integrated-charge distributions with the results of the fits overlaid and (right) corresponding pull distributions for (from top to bottom) different values of integrated charge.

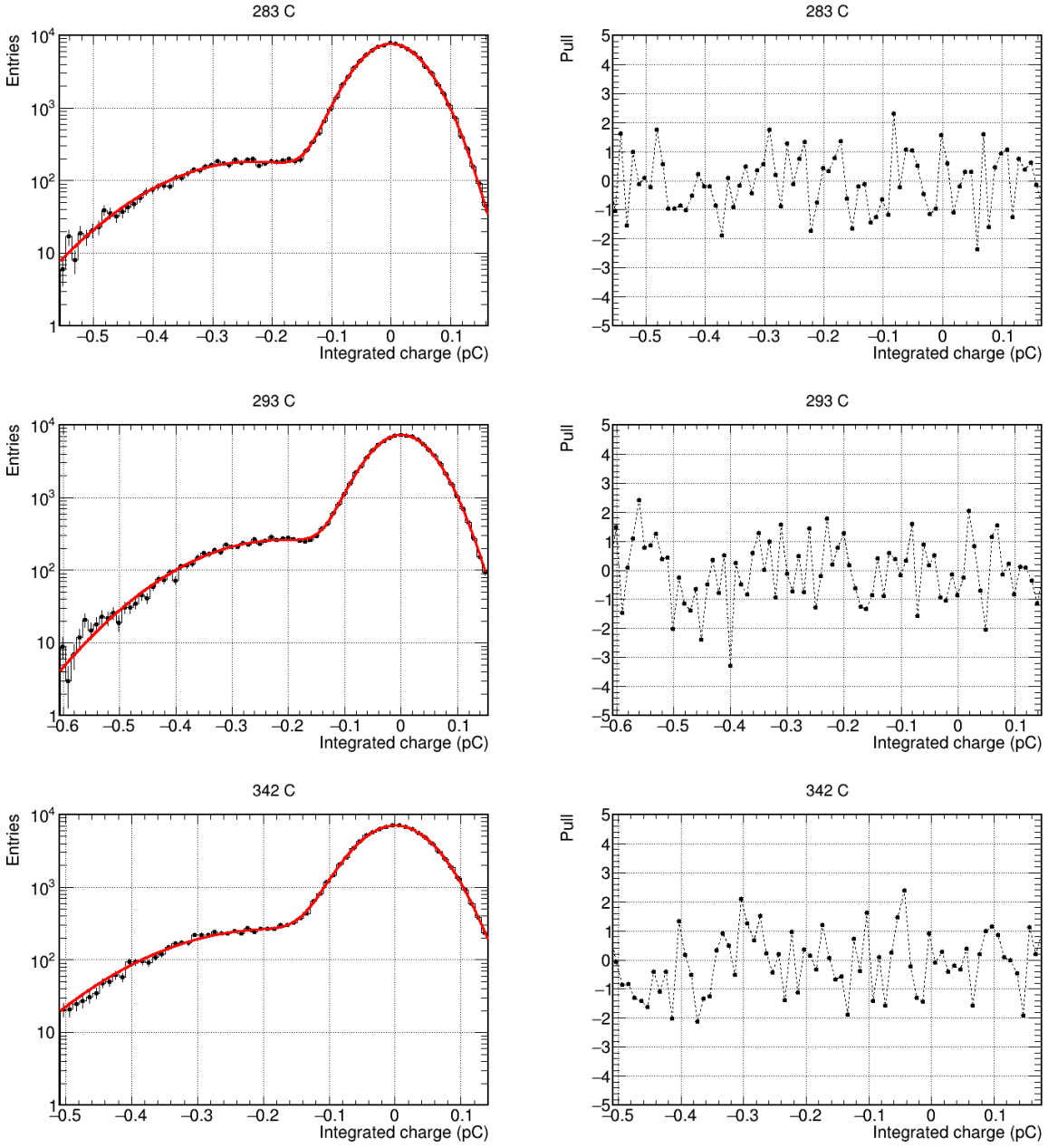

Figure 3.8: (Left) Integrated-charge distributions with the results of the fits overlaid and (right) corresponding pull distributions for (from top to bottom) different values of integrated charge.

3.3 Relative gain

The main purpose of the relative gain measurements is to study the variation of the gain as a function of the high voltage that powers the PMT. In this case, the LED pulse has been switched to 50 MHz with a 20 ns width in order to reach an approximately continuous wave regime and have a constant photons flux hitting the PMT window. The measurements have been performed at seven different high voltages: 1375 V, 1300 V, 1200 V, 1100 V, 1000 V, 900 V and 800 V. The amount of light impinging the PMT photocathode does not depend on the applied voltage and thus, by measuring the anode current for a particular value of HV, one can relate it to the absolute gain measured at 1375 V by using the following relation:

$$G(V) = \frac{G(1375V)}{I(1375V)} \cdot I(V) \tag{3.7}$$

Here, $I(V)$ is the anode current measured using the Philips 2534 system multimeter corresponding to the high voltage V, $I(1375V)$ is the anode current measured at maximum voltage and $G(1375V)$ is the absolute gain obtained thanks to the procedure described in Sec. 3.2. The LED bias is tuned to achieve $I(1375V) \simeq 100$ nA, in order to have detectable currents even when the PMT bias is set to 800 V. Using these measurements, it is possible to study the voltage corrections to apply in order to preserve a fixed value of the PMT gain during its operation.

3.3.1 Measurements

As explained in Sec. 1.5, the expected equation which relates the gain (G) and the high voltage (V) applied to the PMT is of the type given by Eq. (1.14) and can be written as:

$$G(V) = A \cdot V^{\alpha} \tag{3.8}$$

where the exponent α depends on the number n of the amplification stages in the PMT dynode system (which is equal to 10 in this case) and on the structure and materials composing the dynodes, as described in Sec. 1.5. By using this equation as a fit function over the graph including the gain at the seven different high voltages reported above, the fit parameters A and α have been obtained. The experimental data and the results of these fits are shown in Figs. 3.9, 3.10 and 3.11. In each graph, every point has the same relative uncertainty of the absolute gain measurements at 1375 V. All the obtained exponents α as a function of the integrated charge are plotted in Fig. 4.4 and shown in Tab. 4.3 in the next Chapter. They show a initial decrease, followed by fluctuations around a mean constant value, as discussed in Sec. 4.2.

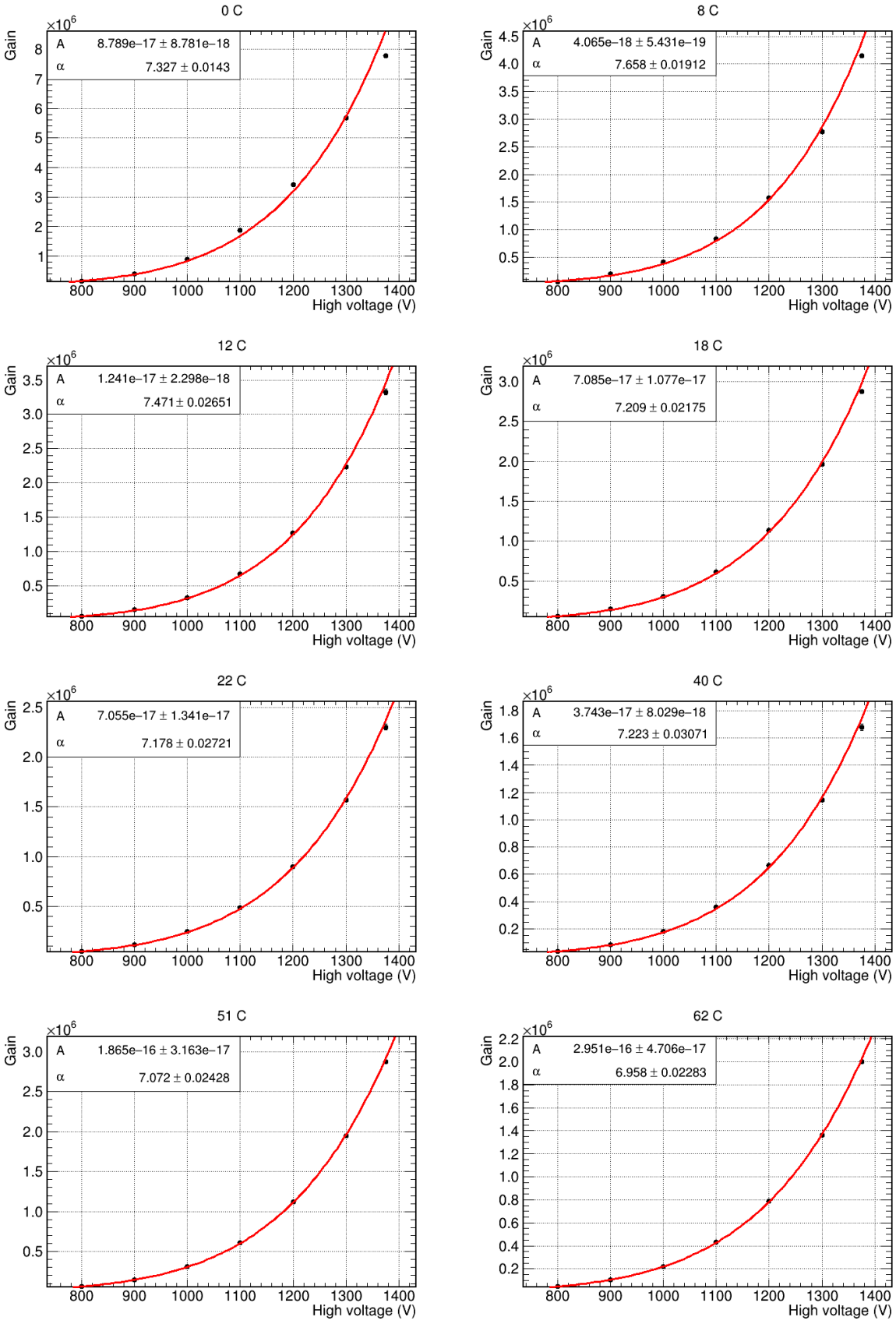

Figure 3.9: Gain as a function of the high voltage applied to the PMT. The data points are obtained from Eq. (3.7) (except for the one at 1375 V) and the fit function is given by Eq. (3.8). The fit parameter A is expressed in $[V^{-\alpha}]$.

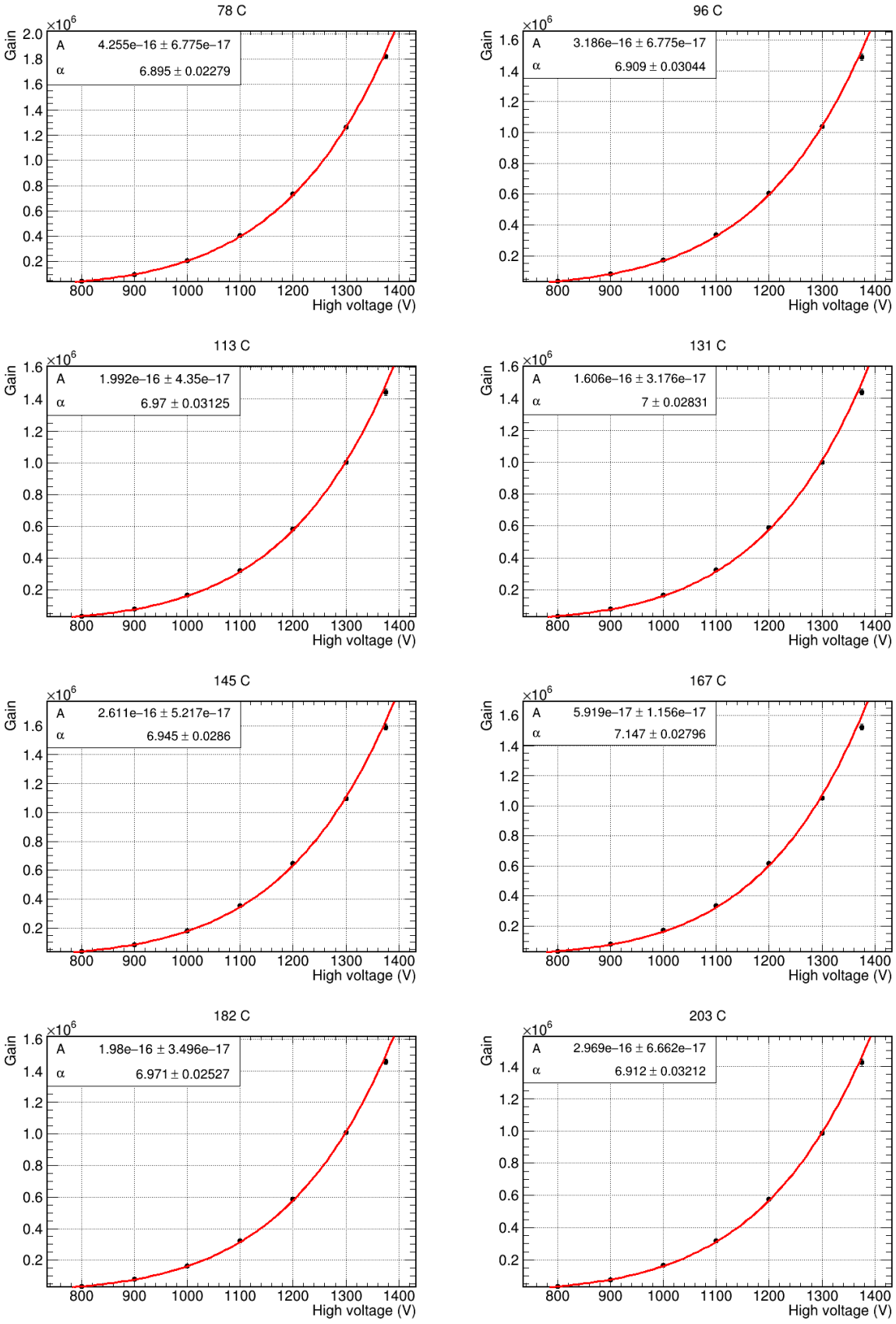

Figure 3.10: Gain as a function of the high voltage applied to the PMT. The data points are obtained from Eq. (3.7) (except for the one at 1375 V) and the fit function is given by Eq. (3.8). The fit parameter A is expressed in $[V^{-\alpha}]$.

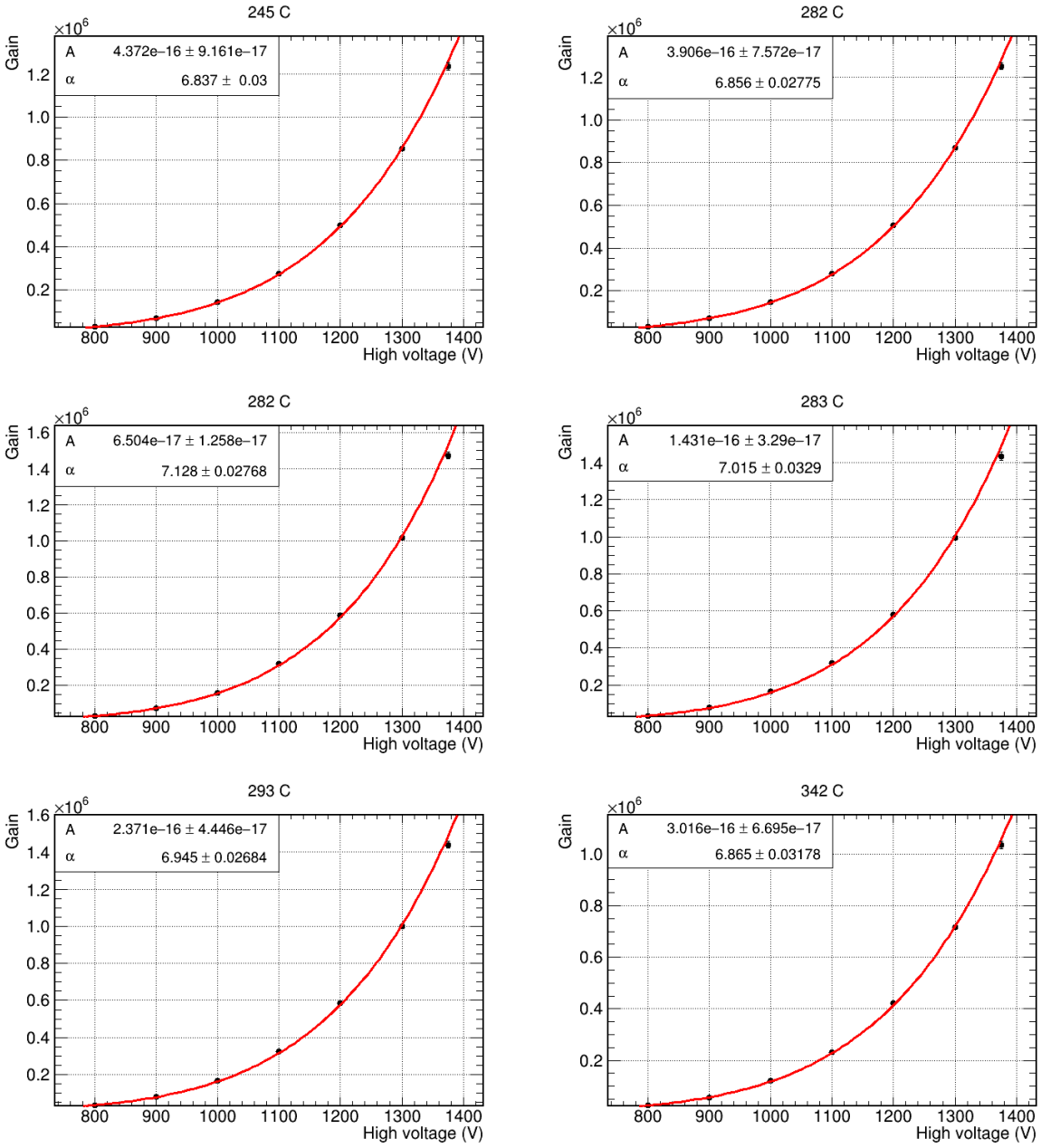

Figure 3.11: Gain as a function of the high voltage applied to the PMT.The data points are obtained from Eq. (3.7) (except for the one at 1375 V) and the fit function is given by Eq. (3.8). The fit parameter A is expressed in $[V^{-\alpha}]$.

Chapter 4

Ageing results

In this Chapter, the main results of the ageing campaign are presented. First, the absolute gain measurements are discussed. They show a quick initial decrease of the PMT gain, followed by a slower one for higher values of integrated charge. Then, the relative gain measurements results are illustrated.

4.1 Absolute gain results

In this section, the consequences of the ageing over the PMT absolute gain measurements are illustrated and discussed in detail, using the experimental data collected during the ageing campaign and presented in Sec. 3.2.1.

Through the best fit parameters in Figs. 3.3, 3.4, 3.5, 3.6 and 3.7, using Eq. (3.5) it has been possible to obtain the gain at increasing integrated charge during the ageing period. The measured gains are shown in Fig. 4.1 and reported in Tab. 4.1 with the corresponding uncertainties and integrated-charge values. They show a quick decrease (almost by a factor of four) during the integration of the first 40 C of charge, followed by a slower one. The latter presents fluctuations around a mean linear decrease, with an angular coefficient $m = (-2180 \pm 54)\,\mathrm{C}^{-1}$ as shown by the linear fit in the bottom part of Fig. 4.1. The recovery period during which the ageing was stopped (between the two values at 282 C) resulted in a small increase of the PMT gain, from $1.25 \cdot 10^6$ to $1.47 \cdot 10^6$. However, this variation is of the same order of the fluctuations around the linear fit function displayed in the bottom part of Fig. 4.1 and thus is not interpreted as a gain recovery after a period of inactivity of the PMT.

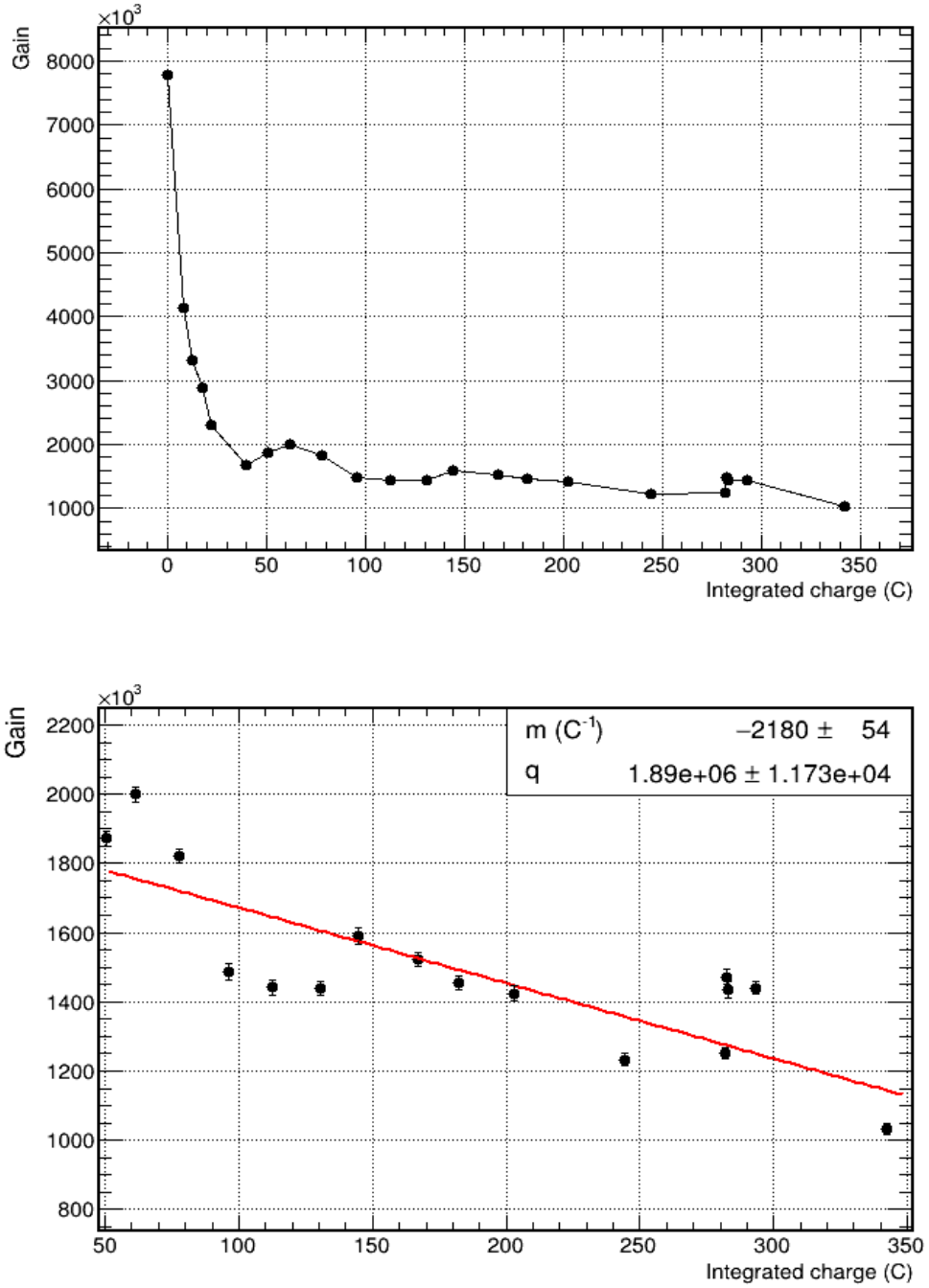

Figure 4.1: Measured gains at 1375 V as a function of the integrated-charge (top) during the whole ageing period and (bottom) in a restricted range, with the result of a linear fit overlaid. The fit function is of the type $f(x) = mx + q$.

Integrated-charge (C)	Gain	Relative uncertainty
0	$(7.786 \pm 0.051) \cdot 10^6$	0.66 %
8	$(4.150 \pm 0.036) \cdot 10^6$	0.87 %
12	$(3.325 \pm 0.041) \cdot 10^6$	1.23 %
18	$(2.878 \pm 0.029) \cdot 10^6$	1.01 %
22	$(2.299 \pm 0.029) \cdot 10^6$	1.26 %
40	$(1.677 \pm 0.024) \cdot 10^6$	1.43 %
51	$(1.874 \pm 0.021) \cdot 10^6$	1.12 %
62	$(1.999 \pm 0.021) \cdot 10^6$	1.05 %
78	$(1.823 \pm 0.019) \cdot 10^6$	1.04 %
96	$(1.487 \pm 0.021) \cdot 10^6$	1.41 %
113	$(1.444 \pm 0.021) \cdot 10^6$	1.45 %
131	$(1.439 \pm 0.019) \cdot 10^6$	1.32 %
145	$(1.589 \pm 0.021) \cdot 10^6$	1.32 %
167	$(1.522 \pm 0.020) \cdot 10^6$	1.31 %
182	$(1.456 \pm 0.017) \cdot 10^6$	1.17 %
203	$(1.423 \pm 0.021) \cdot 10^6$	1.48 %
245	$(1.233 \pm 0.017) \cdot 10^6$	1.38 %
282	$(1.253 \pm 0.016) \cdot 10^6$	1.28 %
282	$(1.472 \pm 0.019) \cdot 10^6$	1.29 %
283	$(1.436 \pm 0.022) \cdot 10^6$	1.53 %
293	$(1.442 \pm 0.018) \cdot 10^6$	1.25 %
342	$(1.033 \pm 0.015) \cdot 10^6$	1.45 %

Table 4.1: Absolute gain measurements with the corresponding integrated charges (expressed in Coulombs) and uncertainties. The recovery period was between the values at 282 C.

4.2 Relative gain results

In this section, the main results of the relative gain measurements discussed in detail in Sec. 3.3 are presented, using the data collected during the whole ageing campaign. First, the variation of the gain at different voltages and the high voltage which has to be applied in order to preserve a gain equal to $1.5 \cdot 10^5$ during the ageing are shown. Then, the behaviour of the parameter α obtained through the fits in Figs. 3.9, 3.10 and 3.11 during the ageing campaign is presented and discussed.

4.2.1 High voltages

During the ageing campaign, the variation of the gain at seven different applied high voltages has been studied.

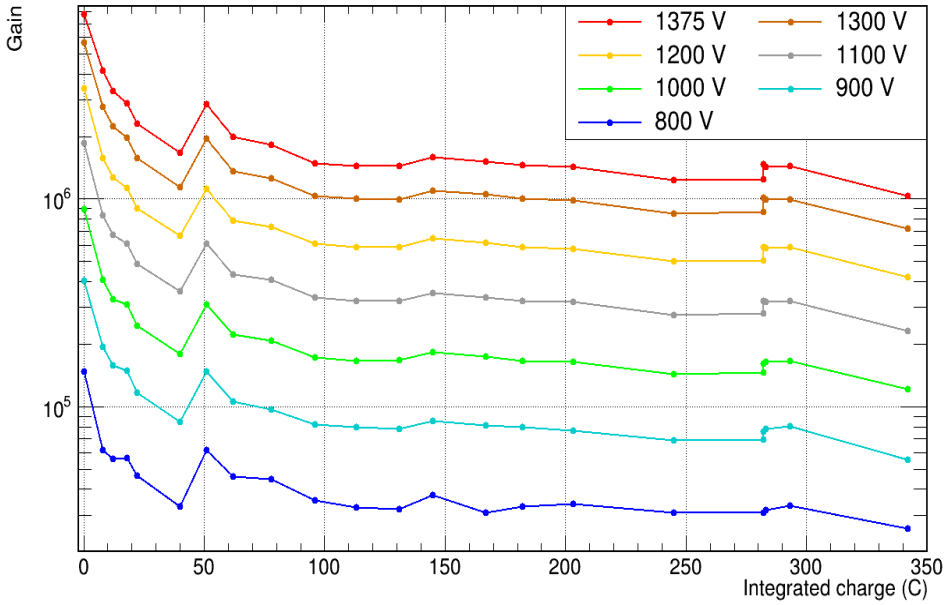

Figure 4.2: Gains as a function of the integrated charge, measured at different fixed high voltages following the "relative method" discussed in Sec. 3.3. The graph is in semi-logarithmic scale.

The experimental data in Figs. 3.9, 3.10, 3.11 are shown in Fig. 4.2 where, for each high voltage applied to the PMT, the gain as a function of the integrated-charge is plotted. There is a similar trend between all the graphs at different voltages, compatible with the one in Fig. 4.1, which corresponds to the red graph at 1375 V. As illustrated in Sec. 3.3, the gain dependence from the high voltage follows a power law, described by Eq. (3.8).

Using the results of the fits in Figs. 3.9, 3.10, 3.11, it has been possible to study the voltage corrections to apply in order to preserve a fixed value of the PMT gain of about $1.5 \cdot 10^5$. The result of this analysis is illustrated in Fig. 4.3 and reported in Tab. 4.2, which show a strong high voltage growth in the first 40 C of integrated-charge, followed

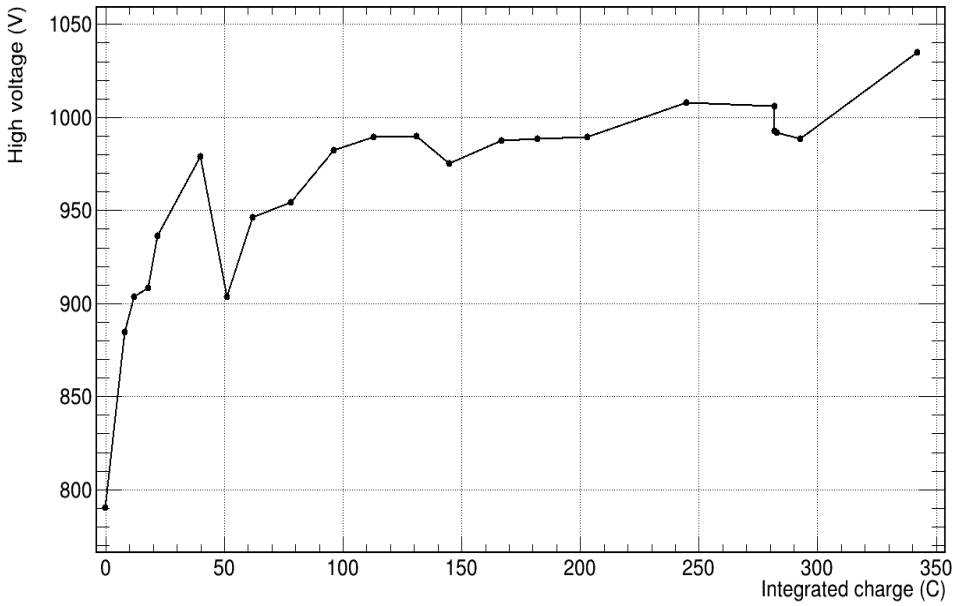

Figure 4.3: High voltage which has to be applied to the PMT in order to reach a gain equal to $1.5 \cdot 10^5$, as a function of the integrated-charge.

by a slower one. This trend is compatible with the graph in Fig. 4.1, since the tendency to decrease of the PMT gain implies a higher voltage which has to be applied in order maintain a costant value of $1.5 \cdot 10^5$. After the recovery period between the two values at 282 C, the high voltage has been subjected to a small decrease from 1006 V to 993 V.

4.2.2 Exponents α

The expected relation between the gain and the applied high voltage is the power law expressed in Eq. (3.8). Here, the main results about the measured exponent parameters α are presented.

All the exponents α obtained from the fits in Figs. 3.9, 3.10 and 3.11 as a function of the integrated charge are plotted in Fig. 4.4. They show an initial decrease, followed by fluctuations around a mean value $\alpha_m = 6.967 \pm 0.007$, obtained by a linear fit (red line in Fig. 4.4) in the range between 50 C and 342 C. After the recovery period (at 282 C), the difference between α and α_m is of the same order of the other fluctuations and thus it is not interpreted as a variation of the parameter value. This trend is compatible with the one of the absolute gain as a function of the integrated charge, illustrated in Fig. 4.1, having a initial decrease followed by a stabilization. As explained in Sec. 1.5, by using Eq. (1.14), the parameter α is given by:

$$\alpha = k \cdot n \tag{4.1}$$

where n is the number of the amplification stages in the PMT dynode system and k depends on the structure and material composing the dynodes. In the case of the Hamamatsu R760 photomultiplier tube under study, there were $n = 10$ dynodes and

Integrated-charge (C)	High voltage (V)
0	790
8	885
12	903
18	908
22	936
40	979
51	904
62	946
78	954
96	982
113	989
131	990
145	975
167	988
182	988
203	990
245	1008
282	1006
282	993
283	992
293	988
342	1035

Table 4.2: High voltage which has to be applied to the PMT in order to reach a gain equal to $1.5 \cdot 10^5$, as a function of the integrated-charge. The recovery period was between the two values at 282 C.

an expected value of k between 0.7 and 0.8 [1], thus the expected fit parameter α was in the range 7–8. Starting from a value $\alpha_i = 7.327 \pm 0.014$ (which is compatible with the expected one), the ageing caused a decrease up to the constant mean value $\alpha_m = 6.967 \pm 0.007$. This decrease is probably caused by the wear of the dynodes emissive layer, described in Sec. 1.6. The obtained values of α are presented in Tab. 4.3.

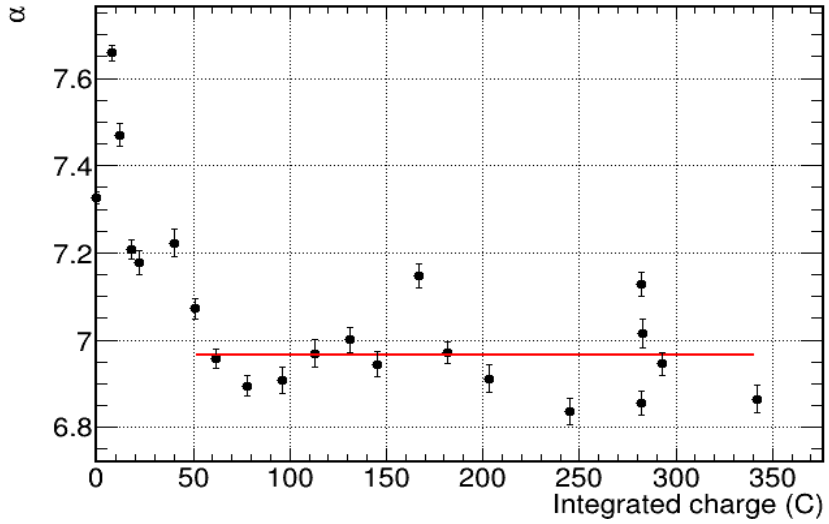

Figure 4.4: Exponent parameter (α) obtained from the fits in Figs. 3.9, 3.10 and 3.11, as a function of the integrated charge, with the result of a linear fit overlaid between 50 C and 342 C.

Integrated charge (C)	α
0	7.327 ± 0.014
8	7.658 ± 0.019
12	7.471 ± 0.027
18	7.209 ± 0.022
22	7.178 ± 0.027
40	7.223 ± 0.031
51	7.072 ± 0.024
62	6.958 ± 0.023
78	6.895 ± 0.023
96	6.909 ± 0.030
113	6.970 ± 0.031
131	7.000 ± 0.028
145	6.945 ± 0.029
167	7.147 ± 0.028
182	6.971 ± 0.025
203	6.912 ± 0.032
245	6.838 ± 0.030
282	6.856 ± 0.028
282	7.128 ± 0.028
283	7.015 ± 0.033
293	6.946 ± 0.027
342	6.865 ± 0.032

Table 4.3: Exponent parameters (α) obtained by the fits in Figs. 3.9, 3.10 and 3.11, with the corresponding integrated charge. The recovery period was between the values at 282 C.

Chapter 5

Conclusions

In this chapter, the main results of the ageing campaign of the Hamamatsu R760 photomultiplier are briefly reported and discussed.

The PMT ageing has been studied from the 22nd of October 2021 to the 21st of January 2022, corresponding to a total integrated charge of 342 C, equivalent to roughly 5 years of LHCb data taking with Run 3 conditions. The campaign featured also a recovery period between the 21st of December 2021 and the 10th of January 2022 (at 282 C of integrated charge), during which the ageing was stopped by turning off the PMT. The PMT high voltage during the ageing was fixed at 1200 V, while in S.P.E. condition it was set to 1375. In order to perform the relative gain measurements, which required different values in order to study the gain dependence from the applied voltage, other high voltages between 1375 V and 800 V have been employed.

The PMT gain represents the amplification factor between the PMT photocathode current and the PMT anode current. It has been measured under the S.P.E. condition described in Sec. 3.1 by fitting the integrated-charge distribution obtained by the integration of the PMT signal, following Eq. (3.4). The model adapted to data considers the cases in which more than one photoelectron (up to five) is emitted from the PMT photocathode, but the fraction of events in which the emitted photoelectrons skipped the first amplification stage of the PMT dynode system has been ignored.

The absolute gain measurements showed a strong decrease during the integration of the first 40 C of charge, starting from $7.79 \cdot 10^6$ and reaching a value of $1.68 \cdot 10^6$. After that, the absolute gain showed smaller variations, consisting in fluctuations around a mean linear decrease, having an angular coefficient $m \simeq -2180$ C^{-1}. These results are illustrated in Fig. 4.1. After the recovery period, the absolute gain variation turned out to be of the same order of the fluctuations reported above. Thus, it has not been interpreted as a relevant PMT gain recovery. To sum up, the campaign revealed that the ageing caused a significant initial decrease of the absolute gain, followed by a slower and approximately linear decrease.

The purpose of the relative gain measurements (discussed in detail in Sec. 3.3) was to study the gain behaviour at different high voltages alimenting the PMT. Thanks to these measurements, it has been possible to obtain the parameters of the power law which relates the gain to the applied voltage (A and α in Eq. (3.8)) through the fits illustrated in Figs. 3.9, 3.10, 3.11. The exponent parameter α showed a quick initial decrease (during the integration of the first 40 C of charge) due to the strong decrease of the PMT gain

reported above, as illustrated in Fig. 4.4. Thus, having a starting value $\alpha_i = 7.327 \pm 0.014$, it finally stabilized around a mean value $\alpha_m = 6.967 \pm 0.007$. Since the measured value of α after the recovery period is of the same order of the other fluctuations around α_m, it has not been interpreted as a relevant variation caused by the stop of the ageing. In the case of the Hamamatsu R760 photomultiplier under study, the expected value for α was between 7 and 8 [1], compatible with the initial parameters. The decrease of the parameter during the ageing was probably caused by the wear of the dynodes emissive layer, as described in Sec. 1.6.

Through the measurements of the PMT anode current, the gain at seven different high voltages (at 1375 V and between 1300 V and 800 V with 100 V steps) has been obtained. The trend of the measured gain as a function of the integrated charge is the same for all the applied high voltages, compatible with the one described in the previous section and in Sec. 4.1.

Since the gain tends to diminish due to the ageing, the high voltage provided to the PMT must be increased in order to maintain the same amplification performances of the PMT dynode system during its operation. Thanks to the relative gain measurements, it has been possible to obtain the high voltage which has to be applied to the PMT in order to reach a gain value equal to $1.5 \cdot 10^5$, as a function of the integrated charge. This value has been chosen as working point for the PLUME sub-detector installed in the LHCb experiment, which will use this PMT model during its operation. Since the PMT gain presented a strong initial decrease followed by a slower one, such high voltage has risen quickly from about 790 V to almost 1000 V in the first 40 C of integrated charge and then has started growing slower, reaching a maximum final value of 1035 V.

The results presented in this thesis will be employed during the PLUME detector operation in order to understand how to change the PMT high voltage as the integrated charge gets accumulated during the LHCb experiment activities.

Bibliography

[1] Hamamatsu Photonics K.K. *Photomultiplier tubes, Basic and Applications*. Third Edition. 2007. URL: https://www.hamamatsu.com/content/dam/hamamatsu-photonics/sites/documents/99_SALES_LIBRARY/etd/PMT_handbook_v3aE.pdf.

[2] Hamamatsu Photonics. URL: https://www.hamamatsu.com/eu/en/product/optical-components.html.

[3] J.H. Hubbel *et al.* "Tables of X-Ray Mass Attenuation Coefficients and Mass Energy-Absorption Coefficients". In: *National Institute of Standards and Technology (NIST)* (1995). URL: https://www.google.it/url?sa=t&rct=j&q=&esrc=s&source=web&cd=&ved=2ahUKEwiZlfKR09_4AhX5QfEDHbGlAnoQFnoECAQQAQ&url=https%3A%2F%2Fnvlpubs.nist.gov%2Fnistpubs%2FLegacy%2FIR%2Fnistir5632.pdf&usg=AOvVaw1b1F_ljcrQliaiyM_S8Xen.

[4] Hamamatsu Photonics. *Photomultiplier tube R*760. URL: https://www.hamamatsu.com/eu/en/product/optical-sensors/pmt/pmt_tube-alone/head-on-type/R760.html.

[5] IJCLab. URL: https://www.ijclab.in2p3.fr/.

[6] L. Cadamuro *et al.* "Characterization of the Hamamatsu R11265-103-M64 multi-anode photomultiplier tube". In: *ArXiv e-prints* (Mar. 2014), p. 15. eprint: 1403.3215.

[7] RCA. *RCA Photomultiplier Manual*. 1970, pp. 49–53.

[8] Thorlabs. 525 *nm LED*. URL: https://www.thorlabs.com/navigation.cfm?guide_id=2101.

[9] Hawlett Packard Company. *HP*-8012*B pulse generator*. URL: https://groups.nscl.msu.edu/nscl_library/manuals/hp/HP-8012B.pdf.

[10] CAEN. 40 *Channel High Voltage System SY*127. URL: http://www.dmf.unisalento.it/~daqatlas/gas_lab/instrumentation/specification/highvoltage/CAEN%20%20Nuclear%20Physics%20%20Products%20%20SY127.htm.

[11] *Philips* 2534 *System Multimeter*. URL: https://www.google.it/url?sa=t&rct=j&q=&esrc=s&source=web&cd=&ved=2ahUKEwj064f7u9_4AhUAQPEDHXMfC7gQFnoECAIQAQ&url=http%3A%2F%2Fbee.mif.pg.gda.pl%2Fciasteczkowypotwor%2FPhilips%2Fpm2534.pdf&usg=AOvVaw1UKs6jz9CfSTpCJSV8RrwZ.

[12] Paul Scherrer Institute. *DRS*4 *Evaluation Board*. URL: https://www.psi.ch/en/drs/evaluation-board.

Acknowledgements

Come conclusione di questa tesi e di questi ultimi tre anni, vorrei ringraziare alcune persone che in un modo o nell'altro sono state di grande aiuto per me.

Innanzitutto, un particolare ringraziamento va al dott. Fabio Ferrari e al Prof. Angelo Carbone, per la grandissima disponibilità, gentilezza e per i consigli ricevuti durante questi mesi di lavoro di preparazione della tesi.

Vorrei ringraziare tutti i miei amici, per le risate e le esperienze di questi ultimi tre anni. In particolare, un ringraziamento va al gruppo dei "Vettori Spurii" e alla Giulia, con i quali ho condiviso tantissime ore di lezione e di studio nell'aula bianca, i laboratori, i pranzi, le birre e tutto il resto.

Infine, un ringraziamento speciale va alla mia famiglia, per il supporto che mi ha sempre dato e per avermi sopportato (credo) anche nei periodi di lockdown e lezioni online.